





0134222

1. Report No. NASA TN D-8522		2. Government Accession No.		3. Recipient's Catalog No.	
4. Title and Subtitle DEVELOPMENT OF A TRANSFER FUNCTION METHOD FOR DYNAMIC STABILITY MEASUREMENT		5. Report Date July 1977		6. Performing Organization Code	
7. Author(s) Wayne Johnson		8. Performing Organization Report No. A-6800		10. Work Unit No. 505-10-22	
9. Performing Organization Name and Address Ames Research Center, NASA and Ames Directorate, USAAMRDL Ames Research Center, Moffett Field, Calif., 94035		11. Contract or Grant No.		13. Type of Report and Period Covered Technical Note	
12. Sponsoring Agency Name and Address National Aeronautics and Space Administration Washington, D. C., 20546 and US Army Air Mobility R&D Laboratory Moffett Field, Calif., 94035		14. Sponsoring Agency Code			
15. Supplementary Notes					
16. Abstract  A flutter testing method based on transfer function measurements is developed. The error statistics of several dynamic stability measurement methods are reviewed. It is shown that the transfer function measurement controls the error level by averaging the data and correlating the input and output. This method also gives the experimenter a direct estimate of the error in the response measurement. An algorithm is developed for obtaining the natural frequency and damping ratio of low-damped modes of the system, using integrals of the transfer function in the vicinity of a resonant peak. Guidelines are given for selecting the parameters in the transfer function measurement. Finally, the dynamic stability measurement technique is applied to data from a wind-tunnel test of a proprotor and wing model.					
17. Key Words (Suggested by Author(s)) Flutter testing Dynamic stability measurement			18. Distribution Statement Unlimited		
19. Security Classif. (of this report) Unclassified		20. Security Classif. (of this page) Unclassified		STAR Category - 01	
				21. No. of Pages 45	22. Price* \$3.75

DEVELOPMENT OF A TRANSFER FUNCTION METHOD  
FOR DYNAMIC STABILITY MEASUREMENT

Wayne Johnson

Ames Research Center  
and  
Ames Directorate, USAAMRDL

SUMMARY

A flutter testing method based on transfer function measurements is developed. The error statistics of several dynamic stability measurement methods are reviewed. It is shown that the transfer function measurement controls the error level by averaging the data and correlating the input and output. This method also gives the experimenter a direct estimate of the error in the response measurement. An algorithm is developed for obtaining the natural frequency and damping ratio of low-damped modes of the system, using integrals of the transfer function in the vicinity of a resonant peak. Guidelines are given for selecting the parameters in the transfer function measurement. Finally, the dynamic stability measurement technique is applied to data from a wind-tunnel test of a proprotor and wing model.

INTRODUCTION

A major task in developing new aircraft is the demonstration of satisfactory aeroelastic characteristics. Beyond the determination of the flutter boundary, or establishing that the aircraft is flutter-free throughout its operating envelope, it is also desirable to obtain detailed dynamic information. This information is used to determine specific characteristics (such as the aircraft gust response) and to verify mathematical models of the aircraft. Thus, the flutter testing of an airplane or helicopter requires an accurate, efficient, and reliable method to measure the aeroelastic response, and then a method to obtain from the response the parameters defining the dynamic characteristics. The most important parameters are generally those defining the flutter stability level, that is, the frequency and damping of the low-damped modes of the system. The state of the art of dynamic stability testing in the aircraft industry has been described in a number of surveys (refs. 1 to 5). The problem usually involved is the flutter testing of the airplane wing or tail in flight. Some form of frequency-response procedure is common. Many variations exist, but a typical procedure involves fast swept-sine excitation, digital analysis of the response (analog analysis is also still common), with the frequency and damping determined from the circle on the phase plane (see ref. 6). Another approach often used is to determine the dynamic stability from the decaying transient response. A number of measurement and analysis techniques has been developed for structural dynamics testing, but in such

testing the principal data required are the frequencies and mode shapes, whereas in flutter testing it is the damping that is of primary concern.

Flutter testing methods such as fast sine sweep or transient decay can work well with clean data. With low process and measurement noise, the excitation level can be sufficiently high that the effects of noise on the measurements can simply be neglected. As the noise increases, however, the accuracy of the flutter parameter determination by such methods degrades rapidly, especially the damping measurement. Dynamic stability measurement is particularly difficult for rotorcraft, where many degrees of freedom are involved, and the levels of process noise (turbulence-induced, especially in a wind tunnel) and measurement noise (rotor- or engine-produced vibration) can be high. Thus, in general, a dynamic stability measurement technique is required that can be applied to data with a significant noise level.

Accurate and reliable flutter testing requires minimal error in measuring system response and in analyzing the data. Regarding control of the error level in the response estimation, the test techniques may be classified in three categories. First are the techniques that use a high signal-to-noise ratio to control the error. Examples are the transient decay method (perhaps using the moving block analysis in the data reduction), and a fast sine-sweep measurement of the transfer function. Second are the techniques that average the estimation of the response due to existing disturbances of the system (such as aerodynamic turbulence). Examples are spectral analysis, correlation, and random decrement signatures. Third are the techniques that, in addition to averaging, use correlation between the response and a measured external input to reduce the error. Examples are single-input, single-output transfer function methods, and more sophisticated parameter identification techniques using several output and input measurements. The error characteristics progressively improve with each of the three categories. After the response measurement is obtained, in either the time or frequency domain, the parameters describing the dynamic characteristics of the system must be calculated, particularly the damping ratio, which gives the quantitative level of stability. A technique is required that is accurate when applied to noisy data and that can be implemented for online stability measurements. Most techniques (including the one developed here) obtain the frequency and damping of the low-damped modes by an algorithm based on the response of a single-degree-of-freedom, second-order system.

In this report, the method for measuring dynamic stability uses a single-input, single-output transfer function, and pays particular attention to the error characteristics with noisy data. The error statistics of several response measurement techniques are summarized to establish the relative value of the transfer function. Then, an algorithm is derived for obtaining the damping ratio and other parameters. Next, the procedure for measuring the transfer function is discussed. Finally, an example of the application of this dynamic stability measurement technique is given. The data used are from a wind-tunnel test of a model proprotor and cantilever wing. We begin with a discussion of the mathematical model used for the aeroelastic system.

The author wishes to thank Professor Norman D. Ham, Paul H. Bauer, and Thomas H. Lawrence of the Massachusetts Institute of Technology for their cooperation in obtaining the experimental data used in this report.

### LINEAR SYSTEM DYNAMICS

A linear system is considered in the examination of the dynamic stability measurement techniques, with excitation by various control inputs and external disturbances. The response of the system is measured, perhaps with significant measurement noise such as rotor- or engine-induced vibration. The system can be excited by existing unknown disturbances (such as aerodynamic turbulence), or by a measurable external input applied to determine the dynamic stability. The system motion is therefore described by linear, time-invariant differential equations, of the form

$$\begin{aligned}\dot{\vec{x}} &= A\vec{x} + B\vec{u} \\ \vec{y} &= C\vec{x} + \vec{v}\end{aligned}$$

where  $\vec{x}$  is the state vector (degrees of freedom), and  $\vec{y}$  is the measurement. The vector  $\vec{v}$  is random measurement noise;  $\vec{u}$  is an input exciting the system, either an existing random disturbance or an external input (random or deterministic). The matrices A, B, and C are constant since the system is time invariant. The solution for the response to excitation by  $\vec{u}$ , with initial conditions at time  $t_0$ , is

$$\begin{aligned}\vec{x}(t) &= e^{A(t-t_0)}\vec{x}(t_0) + \int_{t_0}^t e^{A(t-\tau)} B\vec{u} \, d\tau \\ \vec{y}(t) &= C\vec{x}(t) + \vec{v}\end{aligned}$$

(see ref. 7). The stability of the system is determined by the eigenvalues of A. The eigenvalues usually occur in complex conjugate pairs, of the form

$$\lambda = -\zeta 2\pi\omega_n \pm i 2\pi\omega_n \sqrt{1 - \zeta^2}$$

where  $\omega_n$  is the natural frequency (in Hertz) and  $\zeta$  the damping ratio of the mode. The mode is stable if  $\zeta > 0$ , and is an exponentially decaying oscillation for  $0 < \zeta < 1$ . In flutter testing, the low-damped modes of the system are of primary concern (roughly  $0 < \zeta < 0.1$ ). If  $\Lambda$  is the diagonal matrix of the eigenvalues of A, and M the matrix whose columns are the corresponding eigenvectors, then  $A = M\Lambda M^{-1}$ . For further information on the dynamics of linear systems, the reader is directed to references 7 to 9.

Regardless of the procedure for measuring stability, the system must be controllable and observable. Thus, the input must sufficiently excite the modes of interest and the modes must be observable in the response of the variables measured.

## ERROR ANALYSIS OF THE RESPONSE MEASUREMENT

### Error Analysis of Transient Decay Method

The transient motion of a dynamic system is composed of exponentially decaying oscillations of each mode. A particular measurement is often dominated by one low-damped mode. From the oscillation period and the decay rate of the trace, the frequency and damping of the mode may be estimated. The typical procedure establishes a large sinusoidal motion by external excitation at the natural frequency of the mode of interest. The excitation is stopped and the subsequent transient motion is analyzed to determine the damping.

Consider the linear, time-invariant system described in the previous section, with state variable  $\vec{x}$  and measurement  $\vec{y}$ ;  $\vec{u}$  is process noise, such as aerodynamic turbulence; and  $\vec{v}$  is measurement noise. It is assumed that  $\vec{u}$  and  $\vec{v}$  are random disturbances with zero mean. The motion following time  $t_0$ , where the initial conditions  $\vec{x}(t_0)$  are established by the external excitation, is

$$\vec{y}(t) = Ce^{A(t-t_0)}\vec{x}(t_0) + C \int_{t_0}^t e^{A(t-\tau)} B\vec{u} \, d\tau + \vec{v}$$

The first term in  $\vec{y}$  is the transient we wish to observe. The second term is the noise in the response caused by the disturbances occurring after  $t_0$ . The third term is the measurement noise. The error introduced by these disturbances is the primary difficulty with this technique. The following analysis derives the expected value and variance of the response, designated  $E\vec{y}$  and  $V_y = E(\vec{y} - E\vec{y})^2$ . The terms "expected value" and "variance" are used rather than "mean" and "standard deviation," because the latter are often associated with a time average of the response. Here,  $E\vec{y}$  and  $V_y$  are themselves time-varying quantities. The normalized variance  $\epsilon = \sqrt{V_y}/E\vec{y}$  is the basic error parameter considered. For a discussion of the probabilistic aspects of such an error analysis, see reference 10.

The expected value of the measurement is the transient response  $E\vec{y} = Ce^{A(t-t_0)}\vec{x}(t_0)$ . The external excitation must establish a large, nonzero initial condition for the modes of interest. The variance of the observation is:

$$\begin{aligned} V_y &= E(\vec{y} - E\vec{y})^2 = E(\vec{y}^2) - (E\vec{y})^2 \\ &= C \int_{t_0}^t e^{A(t-\tau)} BQB^T e^{A^T(t-\tau)} d\tau C^T + R \end{aligned}$$

where it is assumed that  $u$  is white noise with correlation  $E\vec{u}(\tau_1)\vec{u}^T(\tau_2) = Q\delta(\tau_1 - \tau_2)$  (so also  $\vec{u}$  for  $t > t_0$  is uncorrelated with  $\vec{x}$  at  $t_0$ ), and the measurement noise covariance is  $R = E[\vec{v}(\tau)\vec{v}^T(\tau)]$ . The steady-state variance  $X = V_x$  of the response of the system to the disturbance  $\vec{u}$  alone is related to  $Q$  by

$$-(AX + XA^T) = BQB^T$$

(ref. 7). If this relation is substituted for  $BQB^T$  in  $Vy$ , then the output variance is proportional to the square of the standard deviation of the steady-state response  $\sigma_x^2 = X$ . In particular, if the response is dominated by a single mode, then the normalized variance is approximately

$$\epsilon^2 = \frac{Vy}{(Ey)^2} \doteq \left(\frac{\sigma_x}{x_0}\right)^2 \left[ e^{-2\lambda(t-t_0)} - 1 \right] + \frac{r}{x_0^2 c^2} e^{-2\lambda(t-t_0)}$$

(see ref. 11). The first term is the process noise; the second term is the measurement noise. As  $t - t_0$  increases and the transient decays, the noise becomes more important. To determine the damping ratio, the transient must be observed while it decays to a fraction  $f$  of the initial value ( $f = 0.3$  to  $0.5$ , typically). The maximum error to be dealt with is thus

$$\epsilon_{\max}^2 \cong \left(\frac{\sigma_x}{x_0}\right)^2 (f^{-2} - 1) + \frac{r}{x_0^2 c^2} f^{-2}$$

which is basically the ratio of the background process and measurement noise, and the smallest value of the transient. The maximum rms error is then at least two to three times the ratio of the rms response due to  $\vec{u}$  and the initial response amplitude, plus the measurement noise.

The frequency and damping from the transient decay are usually based on the response of a single mode

$$x = x_0 e^{-\zeta^2 \pi \omega_n t} \cos(2\pi \omega_n \sqrt{1 - \zeta^2} t + \phi_0)$$

The frequency is given by the period of the oscillation  $\omega = 1/T$  (Hz). To determine the damping ratio, consider two peak amplitude measurements  $x_1$  and  $x_2$ , which are  $n$  oscillations apart. Then, since  $x_2 = x_1 \exp(-2\pi n \zeta / \sqrt{1 - \zeta^2})$ , it follows

$$\zeta = \left[ 1 + \left( \frac{2\pi n}{\ln x_1/x_2} \right)^2 \right]^{-1/2} \cong \frac{\ln x_1/x_2}{2\pi n}$$

Often, this task is accomplished by hand, directly from an oscillograph trace of the response. In general, the damping ratio may be determined from the envelope of the oscillation by  $\zeta \cong -(d \ln x/dt)/2\pi\omega$ . The difficulty in reducing the data lies in determining the envelope of the decaying oscillation.

Another means of analyzing the decaying transient response is the moving block method, which extracts the envelope of the decay. A Fourier transform is applied to a block of data  $y(t)$  from  $t = \tau$  to  $t = \tau + T$ ; the magnitude of the spectrum line at the natural frequency  $\omega_n$ , plotted as a function of  $\tau$ , gives the envelope and hence the damping ratio. Specifically, the operator

$$L = \frac{1}{2\pi} \int_{\tau}^{\tau+T} (\dots) e^{-i2\pi\nu(t-\tau)} dt$$

is applied to the response, yielding the function  $\bar{y}(\tau, \nu) = Ly(t)$ . The magnitude of the expected value of  $\bar{y}$  at the frequency  $\nu = \omega_n$  is proportional to the exponentially decaying envelope

$$|E\bar{y}_{\nu=\omega_n}| \cong \text{constant} * e^{-\zeta 2\pi\omega_n(\tau-t_0)}$$

(see, e.g., refs. 5 or 11). The moving block analysis can also use analog components (a tracking filter locked to the frequency of the desired mode, an rms integrator, and a log converter). The slope of  $\ln|\bar{y}|$  as a function of  $\tau$  gives the damping ratio of the dominant mode in the response. The principal advantage of the moving block analysis is that it extracts the frequency and exponential envelope from the decaying oscillation, which greatly facilitates the mechanization of the data processing task. Working in the frequency domain also reduces the effect of measurement noise, since only noise around the natural frequency  $\omega_n$  is important. However, the moving block analysis involves a linear operator, which can have no fundamental influence on the normalized error (ref. 11). The response of the system to  $\vec{u}$  is mainly a superposition of oscillations at the frequency  $\omega_n$ , which is transmitted through the tracking filter along with the transient oscillation, so the moving block analysis has little effect on the process noise.

Another approach is to curve-fit the measured response to an exponentially decaying oscillation in the time domain. An iterative least-squared-error technique is usually used, and a multimode curve fit may be implemented if necessary. Convergence problems are very likely with a high noise level, however.

A good estimate of the damping can be obtained by the transient decay method with clean data. The moving block or tracking filter analysis helps by mechanizing the extraction of the damping ratio from the data, and by reducing somewhat the measurement noise due to the filtering. The accuracy of the damping estimate degrades rapidly as the noise increases, however. With significant noise, it may be impossible to obtain any meaningful results. Often, the experimenter can do little to control the relative noise in the response measurement either. The error analysis above shows the only options are to increase the amplitude of the initial conditions or to reduce the process and measurement noise. Sometimes the noise can be influenced by the experimenter (e.g., by improving the rotor track or engine isolation to reduce the vibration or by conducting a flight test only under calm atmospheric conditions to minimize the process noise). In a wind tunnel, however, little can be done to reduce the turbulence, which is likely to be high at maximum speed. A substantial increase in the initial excitation is usually not practical either, because of structural or amplitude limitations in both the response and input. Clearly, to handle noisy data adequately, a different test technique is needed.

## Error Analysis of Output Autospectrum Method

To improve the accuracy of the system response measurement, the data must be averaged. One means by which such averaging can be introduced is to measure the response autospectrum. Consider a system excited by a random disturbance, such as aerodynamic turbulence, which is not measured. Let  $S_y^{(k)}(\omega)$  be the autospectrum of the  $k$ th measured time series of the response  $y$ . Then, an estimator of the true spectrum of the response is given by the ensemble average over  $K$  calculations of the spectrum:

$$\hat{S}_y(\omega) = \frac{1}{K} \sum_{k=1}^K S_y^{(k)}(\omega)$$

(ref. 12). The spectrum  $\hat{S}_y$  can be obtained by digital or analog processing. With a digital processor and hardware FFT units, spectrum analysis is more convenient than autocorrelation analysis; also, working in the frequency domain is better suited for data reduction.

Generally, the excitation of the system consists of multiple inputs (e.g., several gust components), so the output spectrum is related to the input spectra by

$$S_y = \sum_i |H_i|^2 S_{v_i}$$

where  $H_i$  is the transfer function between the response  $y$  and the  $i$ th input, and  $S_{v_i}$  is the (unknown) input autospectrum. For the system considered,  $H_i$  is a rational function, with the denominator  $D(\omega)$  - the characteristic equation - the same for all inputs. Thus, with  $H_i = N_i/D$ ,

$$S_y = \sum_i \left| \frac{N_i}{D} \right|^2 S_{v_i} = \frac{\sum_i |N_i|^2 S_{v_i}}{|D|^2}$$

The poles of the characteristic equation, which give the modal frequency and damping, are of primary concern.  $S_y$  is seen to be a direct measure of  $D(\omega)$ . The spectrum  $S_y$  depends also on the characteristics of the input spectra. To obtain the properties of the system alone, the input spectra must be reasonably flat. This criterion is not too severe, since it need be applied only in the vicinity of the resonant peaks, which are very sharp for low-damped modes.

An analysis of the statistics of the estimator  $\hat{S}_y$  of the autospectrum is available in the literature (see refs. 12 and 13). The expected value and variance of  $\hat{S}$  are

$$E\hat{S}(\omega) \cong S(\omega) + \frac{\Delta\omega^2}{24} S''(\omega)$$

$$V\hat{S}(\omega) \cong \frac{S^2(\omega)}{K}$$

where  $\Delta\omega$  is the frequency resolution (in Hz) of the spectrum, and  $K$  the number of averages.<sup>1</sup> These results, which are essentially independent of the statistical properties of the signal, are applicable to general random disturbances. The normalized bias error is

$$\epsilon_b = \frac{\Delta\omega^2 S''}{24S}$$

The most critical case is at a resonant peak, where the greatest accuracy is required and the curvature  $S''$  is largest. Assuming that, in the vicinity of the peak, the spectrum may be approximated by a single-degree-of-freedom system, one obtains  $S/S'' \cong (1/2)\zeta^2\omega_n^2$ . So, for a given bias error, the following frequency resolution is required:

$$\Delta\omega = \sqrt{12\epsilon_b} \zeta\omega_n$$

Using a frequency resolution of  $\Delta\omega = (1/2)\zeta\omega_n$  gives  $\epsilon_b = 0.02$ , which is a negligible bias error compared to the usual variance levels (twice that resolution is often satisfactory). The half-power bandwidth of the peak is  $\Delta\omega_2 = 2\zeta\omega_n$ , so this resolution corresponds to covering the bandwidth of the peak with four or five spectral lines. The sampling time for a single spectrum measurement is related to the frequency resolution (in Hz) by  $T_0 = 1/\Delta\omega$  (ref. 12). Hence, the spectrum frequency resolution is an important test parameter, affecting both the bias error and test time.

The bias error is easily made negligible by a proper choice of the frequency resolution. The remaining error is the normalized variance:

$$\epsilon = \frac{\sqrt{V\hat{S}}}{E\hat{S}} = \frac{1}{\sqrt{K}}$$

This error is inversely proportional to the square root of the number of averages, a standard result for sample means. The estimate of the spectrum may thus be made as accurate as desired by increasing the number of averages. The total record length required for the spectral analysis is the product of the number of averages and the sample time for a single spectrum measurement, which gives

$$T = \frac{K}{\Delta\omega} = \frac{1}{\Delta\omega\epsilon^2}$$

---

<sup>1</sup>If  $N$  samples are collected at rate  $r$ , then the time required to obtain a single record is  $T_0 = N/r$ . The maximum frequency in the spectrum is  $\omega_{\max} = r/2$  (the Nyquist frequency) and the number of spectral lines is  $N/2$ , so the frequency resolution of the spectrum is  $\Delta\omega = r/N = 1/T_0$ . Then, the total sampling time with  $K$  averages is  $T = KT_0 = K/\Delta\omega$ , giving  $K = T\Delta\omega$ , or  $K = TB_e$  in the notation of reference 12.

With the above result for the frequency resolution,  $T = 2/(\zeta\omega_n\epsilon^2)$ ; the total time over which data are collected must be increased as the damping, frequency, or error decreases. This sample time expression is a fundamental result for the amount of data required to estimate the statistics of a random signal. It is thus applicable to all no-input dynamic stability measurement techniques, such as correlation (which is simply a transform of spectral analysis to the time domain) or random decrement analysis (discussed below).

To determine the system properties from the response spectrum, the input spectrum is generally assumed to be flat in the vicinity of each resonance, so  $S_y = |H|^2 S_v \cong |H|^2$ . For the low-damped modes that are of most interest, this assumption is required only over the narrow frequency range  $\Delta\omega/\omega_n \cong 2\zeta$ . Occasionally, the response spectrum can be corrected also for some known variations in the input spectrum. Data reduction then proceeds by treating  $S_y$  as the magnitude of the transfer function. For example, if  $\Delta\omega_2$  is the half-power bandwidth of the resonant peak (where the autospectrum  $S_y \cong |H|^2$  has fallen to one-half the peak value), then the damping ratio can be estimated from  $\zeta = \Delta\omega_2/2\omega_n$ . Alternatively, the damping ratio can be calculated by integrating the spectrum through the resonance

$$\zeta = \frac{1}{\pi\omega_n^3} \frac{\int_0^\infty S_y \omega^2 d\omega}{(S_y)_{\text{peak}}}$$

(This expression can be used to estimate the damping of multimode systems as well by limiting the integration to a narrow range about each resonant peak.)

Spectral analysis, by introducing averaging of the data, gives the experimenter control over the error level in the response measurement. However, techniques that measure only the output have two major difficulties. First, as seen above, the output spectrum depends not just on the system but also on the input characteristics, so there is always some uncertainty whether the system parameters are being correctly estimated. Second, the total record time to measure the spectrum accurately is often impractically long, particularly for full-scale aircraft (which have low fundamental structural frequencies). Consider, for example, a case with  $\omega_n = 5$  Hz,  $\zeta = 0.02$ , and  $\epsilon = 0.2$ ; the above expression gives  $T = 500$  sec.

An autocorrelation analysis is entirely equivalent to an autospectrum analysis, the former working in the time domain and the latter in the frequency domain. The statistics of an autocorrelation measurement are thus similar to the spectrum measurement statistics summarized above (see ref. 13). The method of random decrement signatures (randomdec) is another procedure for analyzing the response of a linear system to unmeasured random disturbances, designed to estimate the transient response of the system. The error statistics of the random decrement method are basically the same as for spectral analysis (see appendix). Spectral analysis, correlation, and random decrement techniques are all members of the general class of methods for analyzing the properties of a system using the response to an unknown random disturbance, with averaging to control the error level. A basic characteristic of such methods is that a large amount of data is required to extract information accurately from the response signal; thus, for low-frequency

systems, the time to collect the data is very long. The examination of the autospectrum measurement method has shown the need for a procedure that is more efficient in reducing the error and that measures the characteristics of the aeroelastic system alone.

### Error Analysis of Transfer Function Method

The accuracy of the measurement of the system response is further improved by measuring the input as well as the output. Beyond the influence of averaging the data, the error is also reduced by the correlation between the input and output; furthermore, the properties of the system alone are obtained, in the form of the transfer function between the output and the input. Usually, a measurable external input is applied specifically to excite the system for the flutter testing. The cross spectrum between the input and output is found, in addition to the autospectra. The ratio of the cross spectrum and the input autospectrum then gives the transfer function  $H(\omega)$ , from which the system parameters may be found.

Consider again a linear system, but now with measurements of both the input and the output:

$$\dot{\vec{x}} = A\vec{x} + B\vec{u} + \vec{w}$$

$$\vec{y} = C\vec{x} + \vec{v}_0$$

$$\vec{z} = \vec{u} + \vec{v}_1$$

Here,  $\vec{u}$  is the random input to the system (which is measured),  $\vec{w}$  is process noise (a random input that is not measured), and  $\vec{v}_0$  and  $\vec{v}_1$  are, respectively, the output and input measurement noise. The measured response is  $\vec{y}$ , and the measured input is  $\vec{z}$ . The noise sources  $\vec{w}$ ,  $\vec{v}_0$ , and  $\vec{v}_1$  are assumed to be unknown random variables with zero mean. The transfer function  $H(\omega)$  is a matrix that defines the response to input at frequency  $\omega$ , that is, for  $\vec{u} = \vec{u}_0 e^{i\omega t}$  the response is  $\vec{y} = H(\omega)\vec{u}_0 e^{i\omega t}$ . Then,

$$H(\omega) = \frac{\vec{y}}{\vec{u}} = C(i\omega - A)^{-1}B$$

(For the applications in this report, only a single input and output are used, so the transfer function is a single function, not a matrix.) Let  $S_{zy}^{(k)}$  be the cross spectrum between  $z$  and  $y$  from the  $k$ th measured time-series of data, and  $S_z^{(k)}$  and  $S_y^{(k)}$  the corresponding autospectra. Then, an estimator of the transfer function  $H(\omega)$  is given by the ratio of the averaged cross spectrum and input autospectrum

$$\hat{H}(\omega) = \frac{\hat{S}_{zy}}{\hat{S}_z} = \frac{\frac{1}{K} \sum_{k=1}^K S_{zy}^{(k)}}{\frac{1}{K} \sum_{k=1}^K S_z^{(k)}}$$

(ref. 12).

An analysis of the statistics of the estimator  $\hat{H}$  is available in the literature (refs. 12 and 13). The variance of the spectra estimators  $\hat{S}_{zy}$  and  $\hat{S}_z$  has been discussed previously for spectral analysis. The statistics of the ratio  $\hat{H}$  are different, however, due to the correlation between the two signals. Bias errors in  $\hat{H}$  are usually much less than the random errors (as long as the frequency resolution is chosen properly), so they will not be discussed. The analysis of the variance of  $\hat{H}$  gives the following result (ref. 12). Let  $\alpha$  be the probability that the magnitude of the difference between the estimate  $\hat{H}(\omega)$  and the true value  $H(\omega)$  is greater than the function  $r(\omega)$ . Thus, with confidence level  $(1 - \alpha)$ ,  $H$  lies with a circle of radius  $r$  about  $\hat{H}$ ,  $|\hat{H} - H| < r$ , where

$$r^2 = \frac{1}{K-1} F_{2,2(K-1);\alpha} (1 - \hat{\gamma}_{zy}^2) \frac{\hat{S}_y}{\hat{S}_z}$$

Here,  $K$  is the number of averages;  $\hat{\gamma}_{zy}$  is the estimate of the input-output coherence function

$$\hat{\gamma}_{zy}^2 = \frac{|\hat{S}_{zy}|^2}{\hat{S}_z \hat{S}_y}$$

and  $F_{2,2(K-1);\alpha}$  is the value of the F-distribution with 2 and  $2(K-1)$  degrees of freedom at the probability level  $1 - \alpha$  (i.e., the probability that  $F > F_{2,2(K-1);\alpha}$  is equal to  $\alpha$ ; see ref. 10). For large  $K$ , the F-distribution may be approximated by  $F_{2,2(K-1);\alpha} = -\ln \alpha$ . Hence, the normalized error of the estimate of the transfer function (note  $|H|^2 = S_y/S_z$ ) is

$$\epsilon^2 = \frac{-\ln \alpha}{K-1} (1 - \hat{\gamma}_{zy}^2)$$

For a confidence level of 95 percent ( $\alpha = 0.05$ ),  $F \cong 3.1$ ; at the 97.5 percent and 99 percent levels,  $F \cong 3.8$  and  $4.8$ , respectively. Assuming a Gaussian distribution, one standard deviation corresponds to a confidence level of 68 percent, which gives  $F = 1.16$ . Hence, except for the effect of  $\hat{\gamma}_{zy}$ , the normalized error would be  $\epsilon^2 \cong 1/K$ , which is the same result as for the variance of the spectra alone.

The coherence function  $\hat{\gamma}_{zy}$  is a measure of how well  $y$  and  $z$  are correlated. With no noise in the system,  $\hat{\gamma}_{zy}$  would be exactly equal to 1.

So,  $1 - \hat{\gamma}_{zy}^2$  is a measure of the effect of noise on the calculation of the response due to a particular input. For the system described above, this factor is approximately

$$\begin{aligned}
 1 - \hat{\gamma}_{zy}^2 &= \frac{\hat{S}_z \hat{S}_y - |\hat{S}_{zy}|^2}{\hat{S}_z \hat{S}_y} \\
 &= \frac{S_u (|H_w|^2 S_w + S_{v_0}) + S_{v_i} S_y}{(S_u + S_{v_i}) S_y} \\
 &\cong \frac{|H_w|^2 S_w}{S_y} + \frac{S_{v_0}}{S_y} + \frac{S_{v_i}}{S_z}
 \end{aligned}$$

The first term is the ratio of the system response due to the process noise and the total response. The last two terms are the ratios of the measurement noise to the signal for the output and input, respectively. When  $\hat{\gamma}_{zy}$  is near unity, which is accomplished by having a high signal-to-noise ratio in the frequency range of interest, the normalized error of the transfer function estimate is reduced much more than with averaging alone. Thus, the number of averages, and so the total measurement time, needed to obtain a specified error level is reduced by correlating the input and output measurements.

The transfer function is thus an accurate and efficient measure of system response. The experimenter controls the error level through the number of averages, and only the properties of the system itself are obtained, since both the input and output are measured. If the input and output are correlated (so the coherence function  $\gamma_{zy}$  is near unity), then the data required to achieve a specified level of accuracy is reduced. (In the experiment discussed later in this report, the amount of data measured would have to be increased by a factor of 10 or 15 to achieve, by averaging alone, the accuracy obtained with the transfer function measurement.) Moreover, with the transfer function method, a quantitative estimate of the error level is available directly from the measured data

$$\begin{aligned}
 \epsilon^2 &= \frac{1.16}{K - 1} \left( 1 - \frac{|S_{zy}|^2}{S_z S_y} \right) \\
 &= \frac{1.16}{K - 1} \left( 1 - |H|^2 \frac{S_z}{S_y} \right)
 \end{aligned}$$

Hence, the dynamic stability measurement technique developed in this report is based on the system transfer function.

## DAMPING RATIO FROM THE TRANSFER FUNCTION

After measuring the transfer function, the experimenter must extract from  $H(\omega)$  the parameters defining the system dynamics, in particular the frequency and damping ratio of the low-damped modes. A method is required to estimate accurately  $\omega_n$  and  $\zeta$  from the data in the vicinity of a resonant peak. This task is not easy because of the rapid variations in the transfer function magnitude and phase near the resonance, and because of the noisy transfer function data. A number of least-squared-error curve-fit techniques was considered (fitting the data to a circle on the phase plane, or to a parabola on the  $\text{Re } H^{-1}$  vs.  $\text{Im } H^{-1}$  plane; or fitting the magnitude of the transfer function  $|H|$  vs.  $\omega$ ). Least-squared-error techniques generally do not work well with noisy data, and so the attempts to develop an algorithm along these lines were not successful. Sometimes a good damping coefficient estimate could be obtained, but usually the results for the damping ratio were poor, even with clean data.

The method adopted for analyzing the transfer function data is based on integrating  $H(\omega)$  through a resonant peak. The use of integrals of the data reduces the sensitivity to noise in  $H$ . Consider the transfer function for a single-degree-of-freedom, second-order system:

$$H = \frac{1}{m(\omega_n^2 - \omega^2) + i C\omega} = \frac{1}{m(\omega_n^2 - \omega^2 + i 2\zeta\omega_n\omega)}$$

where  $\omega_n$  is the natural frequency,  $\zeta$  the damping ratio,  $C$  the damping coefficient, and  $m$  the modal mass. Now

$$\int_0^{\infty} \frac{\omega^2 d\omega}{(\omega^2 - \omega_n^2)^2 + (2\zeta\omega_n\omega)^2} = \frac{\pi}{4\zeta\omega_n}$$

so it follows that the damping ratio is given by

$$\zeta = \frac{1}{\pi\omega_n} \frac{\left( \int_0^{\infty} \text{Im } H\omega d\omega \right)^2}{\int_0^{\infty} |H|^2 \omega^2 d\omega}$$

and

$$C = \frac{-\int_0^{\infty} \text{Im } H\omega d\omega}{\int_0^{\infty} |H|^2 \omega^2 d\omega}$$

The parameters  $\omega_n$  and  $\zeta$  define the eigenvalue of a mode, which is a property of the system as a whole, not of the particular input-output pair considered, while the modal mass and damping coefficient are dimensional parameters that scale with  $y/z$ .

In practice, the system has many degrees of freedom; in any case, the data are available only over a finite frequency range. Thus, the integration is really performed over a finite band around a particular peak:  $\omega = (1 - \Delta f)\omega_n$  to  $\omega = (1 + \Delta f)\omega_n$ , where the bandwidth  $\Delta f$  is a parameter of the algorithm. Then we have

$$\zeta_0 = \frac{1}{\pi\omega_n} \frac{\left[ \int_{(1-\Delta f)\omega_n}^{(1+\Delta f)\omega_n} \text{Im } H\omega \, d\omega \right]^2}{\int_{(1-\Delta f)\omega_n}^{(1+\Delta f)\omega_n} |H|^2 \omega^2 \, d\omega}$$

where the subscript 0 refers to the truncated integral.

In the vicinity of a low-damped resonance, the principal effect of other modes is an overall phase shift. The expression above for the damping ratio was derived for a transfer function having a phase at the peak ( $\omega = \omega_p$ ) of

$$\angle H = -\tan^{-1} \frac{2\zeta\omega_p\omega_n}{\omega_n^2 - \omega_p^2} \cong -90^\circ$$

To apply this expression for  $\zeta$ , it is therefore necessary to rotate the measured transfer function on the phase plane until the phase at the resonant peak is  $-90^\circ$  (see ref. 6). This is accomplished by introducing the following correction when integrating  $\text{Im } H$

$$H_C = H * \frac{-i \overline{H_p}}{|H_p|}$$

where  $H_p$  is the value of the transfer function at the peak (it is not necessary to correct the integral of  $|H|^2$ , of course).

#### Correction for Truncated Integration

The effect of the finite limits of integration is that  $\zeta_0$  is less than the true damping ratio. To correct for the truncation of the integration, let  $\zeta = K\zeta_0$ ; then

$$K = \frac{\int_0^\infty \frac{\omega^2}{D} \, d\omega}{\int_{(1-\Delta f)\omega_n}^{(1+\Delta f)\omega_n} \frac{\omega^2}{D} \, d\omega} = \frac{\frac{\pi}{4\zeta\omega_n}}{\int_{(1-\Delta f)\omega_n}^{(1+\Delta f)\omega_n} \frac{\omega^2}{D} \, d\omega}$$

where  $D = (\omega_n^2 - \omega^2)^2 + (2\zeta\omega_n\omega)^2$ . The integral in  $K$  can be evaluated analytically. Figure 1 shows the function  $K$ , obtained from calculations for various values of  $\zeta$  and  $\Delta f$ ;  $K$  is essentially a function of  $\zeta/\Delta f$  alone (or equivalently,  $\zeta_0/\Delta f$ ). A good approximation, which can be easily implemented, is

$$K \cong 1 + \frac{2}{\pi} \frac{\zeta_0}{\Delta f} + \left(1 - \frac{1}{\pi}\right) \left(2 \frac{\zeta_0}{\Delta f}\right)^4$$

(see fig. 1). The first term is based on an evaluation of  $K$  for small  $\zeta/\Delta f$ ; the second term is added to account for the variation up to about  $\zeta/\Delta f = 2$ . The expression for the damping coefficient  $C$  does not require correction for the finite limits of integration.

### Numerical Integration

The transfer function data are available at discrete frequencies, with separation  $\Delta\omega$ . Evaluating the integrals numerically gives then

$$\int_{(1-\Delta f)\omega_n}^{(1+\Delta f)\omega_n} (\dots) d\omega \cong \sum (\dots) \Delta\omega$$

where the summation extends over the desired frequency range. The trapezoidal rule

$$\int_{\omega_0}^{\omega_1} g d\omega = \frac{\Delta\omega}{2} (g_0 + g_1) - \frac{\Delta\omega^3}{12} g''(\xi), \quad \omega_0 < \xi < \omega_1$$

applied to  $\zeta_0 = (1/\pi)4\zeta^2\omega_n \int (\omega^2/D) d\omega$ , gives the integration error

$$\Delta\zeta_0 \cong -M \frac{\Delta\omega^3}{12} \left(\frac{4\zeta^2\omega_n}{\pi}\right) \left(\frac{\omega^2}{D}\right)''$$

Now, the number of integration steps is  $M = 2\Delta f\omega_n/\Delta\omega$ ; and the integrand curvature is  $(\omega^2/D)'' \cong -1/(2\zeta^4\omega_n^4)$  at the peak. Thus

$$\Delta\zeta_0 \cong \left(\frac{\Delta f}{3\pi}\right) \left(\frac{\Delta\omega}{\zeta\omega_n}\right)^2$$

The required frequency resolution for accurate integration is then

$$\frac{\Delta\omega}{\zeta\omega_n} \cong \sqrt{\frac{3\pi}{\Delta f} \Delta\zeta_0}$$

With  $\Delta f = 0.1$  and  $\Delta\zeta_0 = 0.001$  (a very good bound on the accuracy in calculating  $\zeta_0$ ), the requirement is  $\Delta\omega/\zeta\omega_n \cong 0.3$ . This is expected to be a conservative estimate, since the curvature of the spectrum at the peak is used over the entire range to obtain  $\Delta\zeta_0$ . Indeed, the results of numerical simulations of the algorithm indicate that  $\Delta\omega/\zeta\omega_n \leq 0.7$  is adequate for negligible bias in  $\zeta$  due to the integration error. Recall that the criterion for

negligible bias in measuring the spectra has exactly the same form,  $\Delta\omega/\zeta\omega_n \leq \text{constant}$ . In general, the spectrum estimate bias is the stricter criterion, so satisfying it ensures the accuracy of the numerical integration in the damping ratio algorithm.

### Natural Frequency

The other parameter required to define the eigenvalue is the natural frequency  $\omega_n$ . The data available is the frequency  $\omega_p$  at the resonant peak. The natural frequency  $\omega_n$  is somewhat higher than  $\omega_p$  ( $\omega_n = \omega_p/\sqrt{1 - 2\zeta^2}$ ); moreover, the true peak frequency is not what is available, since the transfer function is known only at points  $\Delta\omega$  apart. Based on the approximation  $|H|^2 = \{2\omega_n^2 m[\zeta^2 + (\omega/\omega_n - 1)^2]\}^{-1}$  near the resonance, a corrected estimate of the natural frequency is

$$\omega_n = \omega_p + \frac{\Delta\omega}{2} \frac{H_p^2(H_R^2 - H_L^2)}{H_p^2(H_R^2 + H_L^2) - 2H_R^2H_L^2}$$

where  $H_p = |H|$  at  $\omega = \omega_p$ , and  $H_{R,L} = |H|$  at  $\omega = \omega_p \pm \Delta\omega$ . Numerical simulations of the damping ratio algorithm show this expression gives  $\omega_n$  quite well.

### Alternative Expressions

If only the magnitude of the transfer function is available, the damping ratio and damping coefficient may be obtained from

$$\zeta = \frac{1}{\pi\omega_n^3} \frac{\int_0^\infty |H|^2 \omega^2 d\omega}{|H_p|^2}$$

and

$$C = \frac{1}{|H_p|\omega_n}$$

where  $|H_p|$  is the value at the resonance peak. The ideal transfer function also gives  $C = -\text{Im } H/|H|^2\omega$  for all frequencies (assuming negligible phase shift due to other modes). These expressions using the transfer function magnitude alone are also useful when the phase is distorted by other modes.

Often, accelerometer measurements are used, rather than displacement or strain gage measurements. The damping ratio calculations may be applied to such data by simply using  $H_a = -\omega^2 H$ , so

$$\zeta = \frac{1}{\pi\omega_n} \frac{\left( \int_0^\infty \frac{\text{Im } H_a}{\omega} d\omega \right)^2}{\int_0^\infty \frac{|H_a|^2}{\omega^2} d\omega}$$

and similarly for the other expressions.

### Damping Ratio Algorithm

In summary, the damping ratio and natural frequency are obtained from the transfer function  $H(\omega)$  as follows. The frequency  $\omega_p$  of a resonant peak is identified by examining the transfer function. Then,  $\omega_n$  and  $\zeta$  are calculated by the following expressions

$$\omega_n = \omega_p + \frac{\Delta\omega}{2} \frac{H_P^2(H_R^2 - H_L^2)}{H_P^2(H_R^2 + H_L^2) - 2H_R^2H_L^2}$$

$$\zeta = \left[ 1 + \frac{0.6366}{\Delta f} \zeta_0 + \frac{0.6817}{(\Delta f/2)^4} \zeta_0^4 \right] \zeta_0$$

$$\zeta_0 = \frac{1}{\pi\omega_n} \frac{\left[ \int_{(1-\Delta f)\omega_n}^{(1+\Delta f)\omega_n} \text{Im } H_C \omega d\omega \right]^2}{\int_{(1-\Delta f)\omega_n}^{(1+\Delta f)\omega_n} |H|^2 \omega^2 d\omega}$$

$$H_C = H * \frac{-i \bar{H}_P}{|H_P|}$$

Similar expressions are given above to calculate the damping coefficient  $C$ , or to use the magnitude of the transfer function alone. Numerical simulations of the algorithm indicate that the calculations are not very sensitive to the choice of the integration bandwidth  $\Delta f$ . Typically, a value  $\Delta f = 0.1$  is used, or less if necessary to avoid a neighboring resonance. (Note that the ratio of the integration bandwidth to the 1/2-power bandwidth equals  $\Delta f/\zeta$ .) Also, the correction for the finite limits of integration is an approximation valid up to about  $\zeta/\Delta f = 2$ , as shown in figure 1. The use of calculations based on the magnitude of the transfer function alone is recommended when a large distortion of the phase is due to other modes, to the extent that no circle on the phase plane exists, even approximately. This is often necessary for the higher modes of a system due to the increased modal density. Otherwise, the integral of the complex-valued transfer function should always be used, since it is less sensitive to noise in the data (particularly in  $|H_P|$ ).

## TRANSFER FUNCTION MEASUREMENT

A typical test setup for the measurement of a system transfer function is shown in figure 2. A random signal generator provides the control input. The signal goes through a bandpass or lowpass filter so that the input energy is concentrated in the frequency range of interest. After establishing the test conditions and setting the signal generator parameters, the input is introduced into the system by increasing the potentiometer setting from zero, while monitoring the input and response. The input level finally established depends on what is required for a good signal-to-noise ratio, on the control actuator limits, and on the limitations of the system response. The potentiometer also quickly but smoothly removes the excitation, if necessary, such as for safety. Having established the excitation of the system, the online data analysis proceeds, beginning with the measurement of the transfer function between the input and some response. (The input signal may also be obtained from a transducer in the system, such as a servo position or load cell. In that case, the transfer function does not include the response of the input mechanism. The original input signal is used mainly when such an input measurement is not available, or when it shows a high level of measurement noise.) After the transfer function is measured, the excitation is removed by turning down the potentiometer. Then, the system parameters are calculated from the transfer function, perhaps while other testing takes place at this condition. After the stability level is obtained, and any significant trends assessed, the test condition may be changed.

The transfer function may be measured in many ways. A digital computer offers great flexibility in obtaining the response data, and is essential for implementing the algorithm for extracting the system parameters from the data, even an algorithm as simple as the one used here. (A special purpose analog or hybrid computer could be constructed to do the job, but with considerable loss in flexibility.) A practical approach is to use a minicomputer system with specialized hardware devices, such as FFT and array processors.

Figure 3 outlines the procedure for measuring the transfer function and calculating the modal frequency and damping according to the algorithm developed in this report. While the random excitation of the system takes place, the selected input and output signals are sampled and digitized at a rate of  $r$ /sec.  $N$  samples are collected for each channel. The discrete Fourier transform is then applied to each of the two blocks of data. It is also convenient at this point to convert the signals to engineering units. From the Fourier transforms of the input and output are obtained the autospectra and cross spectrum of the  $k$ th time series of data. The steps of data collection, Fourier transform, and spectra calculation are repeated  $K$  times, and the spectra averaged over the  $K$  records. Finally, the transfer function is obtained from the ratio of the averaged cross spectrum and the input autospectrum, and the error estimate  $\epsilon$  is calculated according to the expression given earlier. At this point, system excitation may be removed.

Data analysis commences by examining the transfer function and designating the frequency for a particular resonant peak. Then, the natural frequency and damping ratio are calculated, using the algorithm developed above

(the damping coefficient and modal mass may also be calculated if required). This analysis is repeated for all modes observable in the transfer function, and the resulting modal parameters are recorded. Finally, the transfer function, autospectra, and normalized error may be examined and recorded as desired.

The parameters defining the transfer function measurement are the sample rate  $r$ , the sample size  $N$ , and the number of averages  $K$ . The discrete spectra then have  $N/2$  lines, with a maximum frequency  $\omega_{\max} = r/2$  Hz (the Nyquist frequency). Thus, the frequency resolution is  $\Delta\omega = r/N$  Hz. The time required for a single record is  $T_0 = N/r = 1/\Delta\omega$ , and the total test time is  $T = K/\Delta\omega$ . The considerations governing the choice of  $r$ ,  $N$ , and  $K$  will now be discussed (see also refs. 12 and 13).

The sample rate  $r$  should be about 2.5 times the bandwidth of interest. The last 20 percent of the resulting transfer function is therefore disregarded to allow for aliasing. Anti-aliasing filters, with a sharp cutoff at  $\omega_{\max} = r/2$ , should also be used. Generally, the modes of interest should occur roughly in the middle of the spectrum. Data near the maximum frequency are suspect because of aliasing; data near zero frequency are suspect due to bias error. A system with many modes over a wide frequency range can be analyzed in successive runs with different bandwidths and frequency resolutions.

The number of samples  $N$  equals  $r/\Delta\omega$ , so the choice of  $N$  is determined by the required frequency resolution  $\Delta\omega$ . The primary consideration in choosing  $\Delta\omega$  is the bias error in the transfer function. The preceding discussion showed that  $\Delta\omega = (1/2)\zeta\omega_n$  to  $\zeta\omega_n$  is required; the lower limit is usually conservative, so a value near the upper limit is typical. With a resonance in the middle of the spectrum ( $r \cong 4\omega_n$ ), the sample size should be  $N = r/\Delta\omega \cong (4 \text{ to } 8)/\zeta$ , or  $N$  around 400 for a low-damped mode. Typically,  $N = 256$  or  $512$  gives the required frequency resolution. In practice, the required sample size  $N$  should be established by trying two or three values at the beginning of the test, until a value for  $N$  is found that gives no noticeable bias error in  $H(\omega)$  (the resonant peak amplitudes are the primary criterion).

The final parameter chosen is the number of records  $K$ , or equivalently the total data collection time  $T$ . In general, as many averages as possible are desired for the smallest error level; if necessary, the number of samples  $N$  could be reduced to shorten the test time. The averages required should be established by trying several values early in the test, and examining the error level as indicated by the normalized error  $\epsilon$ , noise in  $H(\omega)$ , and variations in the resulting parameters (especially the damping ratio). For a full-scale aeroelastic system, with low fundamental frequencies, the number of averages used is normally a compromise between what one would like for very low error and the requirements of an acceptable total test time. The more information that can be obtained from the data, the greater the justification for a longer test time.

## EXAMPLE OF APPLICATION

To demonstrate the application, the transfer function dynamic stability measurement technique was used in the flutter testing of a proprotor and cantilever wing model in a wind tunnel (fig. 4). The three-bladed, gimbaled stiff-inplane rotor had a diameter of 0.86 m, and was operated at a speed of  $\Omega = 22.67$  Hz (1360 rpm). The model was unpowered and hence was operating in a windmilling condition. The model was tested in the MIT Wright Brothers Wind Tunnel in axial flow over a speed range of  $V/\Omega R = 0.34$  to 0.69 (where  $V$  was the forward speed and  $\Omega R$  was the rotor tip speed). The rotor controls consisted of collective and cyclic pitch actuators. The pylon also had a shaker vane (see fig. 4) that was used to excite the wing bending; the shaker vane was equivalent in effect to a wing flaperon. The fundamental wing frequencies were approximately 8.2 Hz (0.36/rev) for vertical bending, and 12.5 Hz (0.55/rev) for chordwise bending. ("Vertical" bending refers to the wing motion on the airplane, not to the orientation used in the wind-tunnel test.) Basically, the shaker vane was used to excite the wing vertical bending mode, and rotor collective pitch was used to excite the wing chordwise bending mode. Rotor cyclic excitation was also tried. Reference 14 gives complete details of the model.

The proprotor and cantilever wing configuration is characterized by an aeroelastic instability at high inflow ratio due to the coupled motion of the rotor and wing. Thus, with this model, it was necessary to measure the frequency and damping of the fundamental wing modes, vertical and chordwise bending, as a function of tunnel speed. What was desired in such a test was sufficient accuracy to detect trends in the stability so that the flutter boundary could be avoided, and enough information to allow correlation with stability predictions. Figure 5 shows typical results of the transient decay technique for this model. A scatter in the damping ratio data of  $\Delta\zeta = 0.01$  or more was characteristic, so little useful information could be obtained with this method. The difficulty, which is typical of wind-tunnel testing, was that the response to tunnel turbulence obscured the transient, especially at high speed where the flutter measurement was most critical. Often there are more degrees of freedom involved than with this model, which makes it more difficult to produce and interpret the transient decay traces. Thus, the transfer function technique was used with this model to control the error level and thus obtain sufficiently accurate measurements of the system damping.

Figure 6 shows the time history and autospectrum of the input signal used to measure the system transfer function. The input was white noise sent through a 3 to 12 Hz bandpass filter. Figure 7 gives the corresponding rms levels of the shaker vane and collective pitch used to excite the system. The level used was determined by the requirements for a significant response level, and the limitations on blade and wing loads. The shaker vane rms excitation was 1.5 to 2 deg, and the collective pitch was 0.25 to 0.75 deg; cyclic pitch was also used, at a level of about 0.25 deg (the cyclic pitch input was limited by an infinite-life blade load restriction). The one-half peak-to-peak level was around 3 to 4 times the rms value. These various control inputs were applied not simultaneously, but in sequential test points. Figure 8 shows the resulting time histories of the wing and rotor motion,

comparing the cases with and without the external excitation (at  $V/\Omega R = 0.69$ ). Figure 9 gives the corresponding rms levels of the wing vertical and chordwise bending response (or one-half peak-to-peak, which is 3 or 4 times the rms level; only the relative values with and without the input are of concern here). The wing response with external excitation, used in the measurement of the transfer function, was 2 or 3 times the response due to the existing tunnel turbulence (the process noise). Generally, the actual control position was used as the input measurement but, for a couple of the collective excitation points, it was necessary to use the original signal to the actuator. Figure 10 shows the transfer functions of the rotor and shaker vane control actuators (the response magnitude has a linear scale). The rotor control actuators had a response flat enough that it need not be considered in obtaining the system transfer function.

The model was tested at four speeds by successively exciting the shaker vane, rotor collective, and rotor cyclic pitch controls. The input (control position) and output (wing bending) signals were sent through 25 Hz low-pass, anti-aliasing filters. The signals were sampled at a rate of  $r = 51.2$  Hz, with  $N = 512$  samples collected for a single record. The spectra were averaged over  $K = 17$  to 20 records. Thus, the spectra bandwidth was  $\omega_{\max} = 25.6$  Hz; the frequency resolution,  $\Delta\omega = 0.1$  Hz; the time for a single record,  $T_0 = 10$  sec; and the total data collection time,  $T = 170$  to 200 sec. The damping ratio calculation used  $\Delta f = 0.1$ . Figures 11 to 13 present the measured transfer functions at the four speeds, for, respectively, wing vertical bending response to shaker vane, chordwise bending response to collective, and vertical bending response to cyclic. The vertical scale of the transfer function magnitude is linear. The resonances of the fundamental wing modes are clearly evident. The scales of the transfer function magnitude plots are not the same in a given figure; the dimensional magnitude is not relevant for the present purposes anyway. Figure 14 gives examples of the transfer function on the phase plane ( $\text{Re } H$  vs.  $\text{Im } H$ ); the circle is characteristic of a low-damped resonance. Figure 15 shows the transfer function error estimates obtained from the data. The number of averages  $K = 17$  to 20 gives a basic error level of  $\epsilon \approx 0.25$ . The lower values of  $\epsilon$  observed in figure 15 are the result of correlation between the input and output; the reduction in  $\epsilon$  occurs where there is a significant input level. To obtain this error level by averaging alone would require 10 or 15 times the data collected here, which would require a prohibitively long test time, even for a small-scale model. The efficiency of the transfer function measurement is clear.

Finally, figure 16 presents the frequency and damping of the two wing modes obtained from the transfer function measurement by the algorithm developed in this report. For the wing vertical bending, two measurements of the damping are available: from the shaker vane and rotor cyclic pitch excitation. At high speed, the shaker vane results are considered more accurate, as indicated by the line connecting the data in figure 16. This choice is based on the transfer function error levels found at high speed, as shown in figure 15. The cyclic transfer function shows a high error (due to limitations on the cyclic input level), while at low speed it shows an effect of the input-output correlation similar to that observed in the shaker vane transfer function.

This is an excellent example showing how the transfer function method cannot only control the error level but also directly assess it, and thus allow the experimenter to determine directly the most accurate measurements.

#### CONCLUDING REMARKS

The error statistics of several dynamic stability measurement techniques have been reviewed. The value of the transfer function measurement lies in the capability it gives the experimenter to control the error level, through averaging of the data and correlation between the input and output. Thus, a satisfactory error level may be achieved with a practical total test time. The characteristics of the system alone are obtained, independent of the input statistics (assuming an adequate bandwidth of the input spectrum). Moreover, the measured data give directly a quantitative estimate of the normalized error in the transfer function, which is extremely important in assessing the quality of the data. Thus, the transfer function is the basis for an accurate and efficient measurement of the system characteristics. An algorithm for obtaining the modal frequency and damping from the transfer function has been developed. The development of the test technique concluded by summarizing the rules for selecting the parameters involved in the transfer function measurement.

The method developed here has two principal limitations. First, only a single-input, single-output transfer function was considered. Second, the data reduction algorithm is based on the response of a single-degree-of-freedom, second-order system; so, for multimode systems it is generally limited to analyzing the fairly low-damped modes. That is the most important information for flutter testing, but still the algorithm is only approximate, and the resulting information about the system is not complete. These limitations are fairly common in flutter-testing techniques. Therefore, a further development of the data reduction procedures would be desirable. The transfer function would still remain the basis of the stability measurement, providing the fundamental error control. The analysis procedure should handle multi-output, multi-input data; and it should completely and accurately identify all the poles and zeros of the system. Such a parameter identification algorithm would require more computational flexibility for the data analysis than the algorithm in this report. The major difficulties lie in developing an algorithm that accurately and efficiently obtains the system parameters from noisy data and that is still applicable for on-line analysis in flutter testing.

The assumptions inherent in the use of a transfer function representation are that the system is linear and time-invariant. These assumptions are quite satisfactory in practice, but time-invariance leads to further problems with rotorcraft testing. To have a time-invariant (constant coefficient) system often requires nonrotating degrees of freedom representing the rotor motion, which in turn requires that the motion of all the rotor blades be measured. Such complete measurements are seldom available; usually, only one blade is instrumented. What is required in such cases is a filter (i.e., an output error estimation method) that estimates the nonrotating states of the rotor

from measurements of the individual blades in the rotating frame, especially with data from only one or two of the blades. Then, the transfer function methods may be applied.

Ames Research Center  
National Aeronautics and Space Administration  
and  
Ames Directorate, USAAMRDL  
Moffett Field, Calif., 94035, April 1, 1977.

## APPENDIX

### ERROR ANALYSIS OF THE METHOD OF RANDOM

#### DECREMENT SIGNATURES

The method of random decrement signatures (randomdec) is a procedure developed by Cole (ref. 15) for analyzing the response of a linear system to random disturbances. The procedure is designed to estimate the transient response of the system. This appendix analyzes the error statistics of the random decrement signatures. The randomdec estimator  $\bar{y}$  is defined as the ensemble average of the response to existing random disturbances

$$\bar{y}(t) = \frac{1}{K} \sum_{k=1}^K \vec{y}_k(t)$$

As usual, the ergodic hypothesis is used, and the random decrement signature is obtained by averaging records that are sequential in time

$$\bar{y}(t) = \frac{1}{K} \sum_{k=1}^K \vec{y}(t + t_0^{(k)})$$

The records are assumed to be uncorrelated, which is generally true if there is no overlap (ref. 15). The key to the procedure is to select each ensemble  $\vec{y}_k$  with the same initial conditions by an appropriate triggering method. Then, all records have an identical transient due to the initial conditions, while the subsequent noise averages out.

Consider again the linear system  $\dot{\vec{x}} = A\vec{x} + B\vec{u}$ , and response measurement  $\vec{y} = C\vec{x} + \vec{v}$ , excited by the unknown random disturbance  $\vec{u}$ , with measurement noise  $\vec{v}$ . Assume that  $\vec{u}$  and  $\vec{v}$  have zero mean. The solution using the initial conditions at time  $t_0$  is

$$\vec{y} = Ce^{A(t-t_0)}\vec{x}(t_0) + C \int_{t_0}^t e^{A(t-\tau)} B\vec{u} \, d\tau + \vec{v}$$

The observation  $\vec{y}(t)$  is thus a random process, depending on the random variables  $\vec{u}$ ,  $\vec{v}$ , and  $\vec{x}(t_0)$ . The expected value of the random decrement signature is then

$$E\bar{y} = \frac{1}{K} \sum_{k=1}^K E\vec{y}_k = Ce^{A(t-t_0)}\vec{x}_0$$

Here, the initial condition  $\vec{x}(t_0)$  is a stationary random variable with expected value  $\vec{x}_0 = E\vec{x}(t_0)$ . Hence,  $\bar{y}$  is an unbiased estimator of the system

transient response. It also follows that  $\bar{y}$  depends on the trigger procedure, which determines  $\vec{x}_0$ . Clearly, the frequency content of the random disturbance  $\vec{u}$  must be sufficient to excite the modes of interest, for  $\vec{x}_0$  must be selected from the steady-state response to  $\vec{u}$ . Moreover, the trigger process must be such that there are nonzero initial conditions for the modes of interest. The usual procedure is to trigger the start of the ensemble on a fixed, nonzero level of the response  $y$ , with either positive or negative slope. Cole (ref. 15) suggests a trigger level of  $y = 1.0$  to  $1.6 \sigma_y$  (where  $\sigma_y$  is the rms level of the response).

The variance of the random decrement signature  $\bar{y}$  is

$$\begin{aligned} V\bar{y} &= E\bar{y}^2 - (E\bar{y})^2 \\ &= C e^{A(t-t_0)} V_{x_0} e^{A^T(t-t_0)} C^T \\ &\quad + \frac{1}{K} \left[ C \int_{t_0}^t e^{A(t-\tau)} B Q B^T e^{A^T(t-\tau)} d\tau C^T + R \right] \end{aligned}$$

Here, it has been assumed that  $u$  and  $v$  are uncorrelated; that the measurement noise covariance is  $R$ ; and that the excitation  $\vec{u}$  is white noise with  $E\vec{u}(\tau_1)\vec{u}^T(\tau_2) = Q\delta(\tau_1 - \tau_2)$ . The ensembles are uncorrelated, except for the initial conditions. The triggering process determines  $\vec{x}(t_0)$ , with expected value  $\vec{x}_0 = E\vec{x}(t_0)$ , and variance  $V_{x_0} = E\vec{x}(t_0)\vec{x}^T(t_0) - \vec{x}_0\vec{x}_0^T$ . (The steady-state response of the system to the disturbance  $\vec{u}$  has zero mean and variance  $\sigma_x^2 = E\vec{x}(t)\vec{x}^T(t)$ , which is not the same as  $\vec{x}_0$  and  $V_{x_0}$  due to the procedure for selecting the initial time  $t_0$ .) The second term in  $V\bar{y}$  is the same error as found for the transient decay, divided by the number of averages  $K$ . It follows that for a signature with a transient that decays to a fraction  $f$  of its initial value, this term gives a maximum error approximately

$$\epsilon^2 = \frac{1}{K} \left[ \left( \frac{\sigma_x}{x_0} \right)^2 (f^{-2} - 1) + \frac{r}{x_0^2} f^{-2} \right]$$

(cf. the analysis above for transient decay). So, the ensemble averaging reduces the error in the transient due to the response of the system to the random disturbance  $u$  subsequent to the time  $t_0$  where the initial conditions are determined. As usual, the error is inversely proportional to the square root of the number of averages. This error source can be made as small as required by increasing the number of averages. (Here, the experimenter does not have control of  $\sigma_x/x_0$ , since  $x_0$  must be obtained from the time series with rms level  $\sigma_x$ ; generally,  $\sigma_x/x_0 \cong 0.5$  to  $1$ .)

The remaining term in  $V\bar{y}$  depends upon the variance of the initial conditions  $V_{x_0}$ . Both this term and  $(E\bar{y})^2$  decrease with time at the same rate, so the normalized error in  $\bar{y}$  always has about the same value, equal to the normalized error in  $\vec{x}(t_0)$

$$\epsilon^2 = \frac{V\bar{y}}{(E\bar{y})^2} \cong \frac{Vx_0}{x_0^2}$$

The ensemble averaging does not affect this term, so an accurate response measurement depends upon keeping the variance of  $\vec{x}(t_0)$  as low as possible. The triggering process is required to select  $t_0$  based on the measurement of  $y$ , such that  $\vec{x} = \vec{x}_0$ . An error in  $\bar{y}$  results unless exactly the same initial conditions are produced by every triggering event. The sources of the variance  $Vx_0$  include: variation in the trigger mechanism or algorithm; several modes observable in  $y$ ; and measurement noise in  $y$ . The measurement noise is probably the most important problem; with a trigger based on  $y$ , the measurement noise covariance must give a lower bound on  $Vx_0$ . With high measurement noise, the experimenter can do little to control the error in the random decrement signature estimate of the transient response. Increasing the number of averages does not influence this error; the trigger level cannot be increased much without increasing the correlation of the records (ref. 15); and it is not often possible to increase the excitation  $\vec{u}$  relative to the measurement noise  $\vec{v}$ .

Finally, consider the total amount of data required. The time for a single record, with decay to a fraction  $f$  of the initial value, is  $T_0 = -\ln f / (2\pi\zeta\omega_n)$ . Then, assuming that the  $Vx_0$  error is negligible, the total sample time required is

$$T = KT_0 = \frac{\text{constant}}{\zeta\omega_n\epsilon^2}$$

This is the same result as for spectral analysis (allowing for a somewhat different meaning of  $\epsilon$ ; see also ref. 15). It is the general result for the amount of data required to estimate the statistics of a random signal. As for spectral analysis, for a given  $T$  it is necessary to compromise between frequency resolution and the number of averages. Typical applications of the random decrement signature procedure require  $K = 2000$  to  $8000$  averages for satisfactory accuracy (refs. 15 and 16). Data processing for the randomdec method follows the lines discussed for obtaining the damping from a transient decay trace, with improved accuracy due to the ensemble averaging. Analysis in the time domain is rather more sensitive to noisy data than analysis in the frequency domain, but it has been successfully implemented in practice.

As with autospectral analysis, there are two basic difficulties with the method of random decrement signatures. First, there is some uncertainty whether only the properties of the aeroelastic system are being estimated (because only the system output is measured). In particular, the initial condition variance is an error source that can neither be controlled by averaging nor be estimated directly from the experimental data. Second, the total measurement time required to obtain accurate estimates of the system properties is likely to be very long. This large amount of data required to extract information accurately from the signal is the basic characteristic of the class of methods utilizing response measurements alone. For further discussion for the random decrement statistics, see reference 11.

## REFERENCES

1. Proceedings of the 1958 Flight Flutter Testing Symposium, Washington, D. C., NASA SP-385, 1958.
2. Baird, E. F.; and Clark, W. B.: Recent Developments in Flight Flutter Testing in the United States. AGARD Report No. 596, Dec. 1972.
3. Rosenbaum, Robert: Survey of Aircraft Subcritical Flight Flutter Testing Methods. NASA CR-132479, 1974.
4. Houbolt, John C.: Subcritical Flutter Testing and System Identification. NASA CR-132480, 1974.
5. Proceedings of NASA Symposium on Flutter Testing Techniques, Dryden Flight Research Center, Edwards, California, NASA SP-415, Oct. 1975.
6. Kennedy, Charles C.; and Pancu, C. D. P.: Use of Vectors in Vibration Measurement and Analysis. J. Aeronaut. Sci., vol. 14, no. 11, Nov. 1947, pp. 603-630.
7. DeRusso, Paul M.; Roy, Rob J.; and Close, Charles M.: State Variables for Engineers. John Wiley and Sons, Inc., 1965.
8. Greenwood, Donald T.; and Yung, F., eds.: Principles of Dynamics. Prentice-Hall, 1965.
9. Hurty, Walter C.; and Rubinstein, Moshe F.: Dynamics of Structures. Prentice-Hall, 1964.
10. Brunk, H. D.: An Introduction to Mathematical Statistics. Second ed. Blaisdell Publishing Co., N. Y., 1965.
11. Johnson, Wayne: A Discussion of Dynamic Stability Measurement Techniques. NASA TM X-73,081, 1975.
12. Bendat, Julius S.; and Piersol, Allan G.: Random Data: Analysis and Measurement Procedures. Wiley-Interscience, N. Y., 1971.
13. Jenkins, Gwilym M.; and Watts, Donald G.: Spectral Analysis and Its Applications. Holden-Day, San Francisco, 1968.
14. Ham, Norman D.; Bauer, Paul H.; Lawrence, Thomas H.; and Yasue, Masahiro: A Study of Gust and Control Response of Model Rotor-Propellers in a Wind Tunnel Airstream. NASA CR-137756, 1975.
15. Cole, Henry A., Jr.: On-Line Failure Detection and Damping Measurement of Aerospace Structures by Random Decrement Signatures. NASA CR-2205, 1973.
16. Chang, C. S.: Study of Dynamic Characteristics of Aeroelastic Systems Utilizing Randomdec Signatures. NASA CR-132563, 1975.



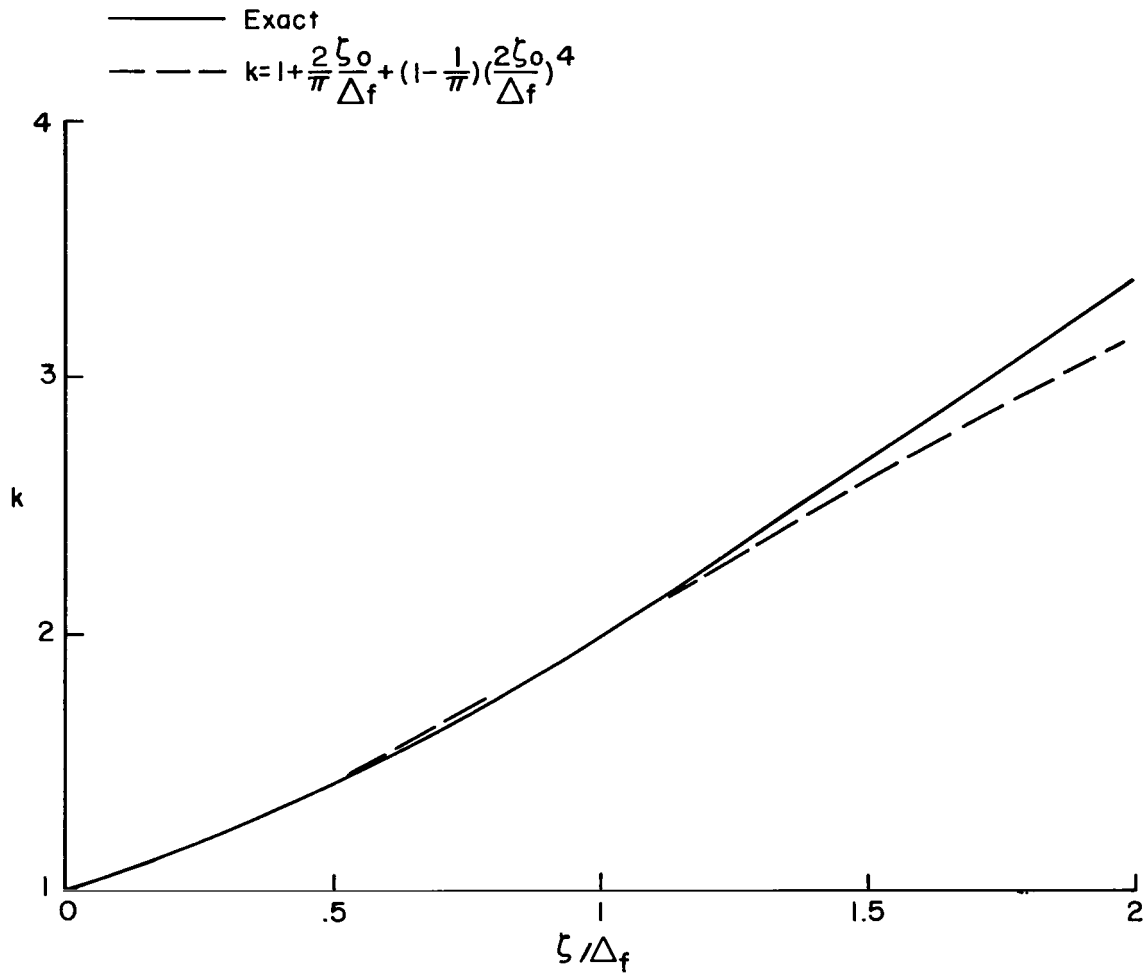


Figure 1.- Correction of integral in damping ratio calculation for finite limits of integration;  $\zeta = K_0$ .

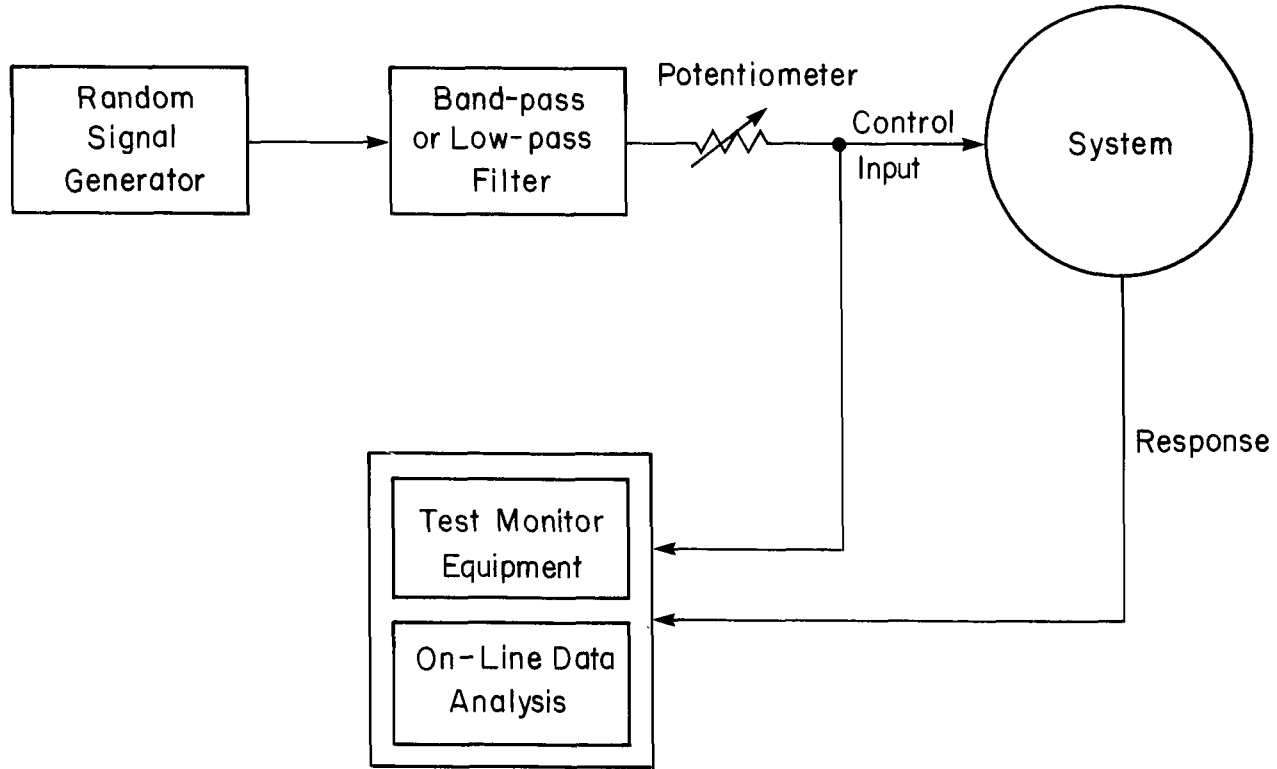


Figure 2.- Typical test setup to measure system transfer function.

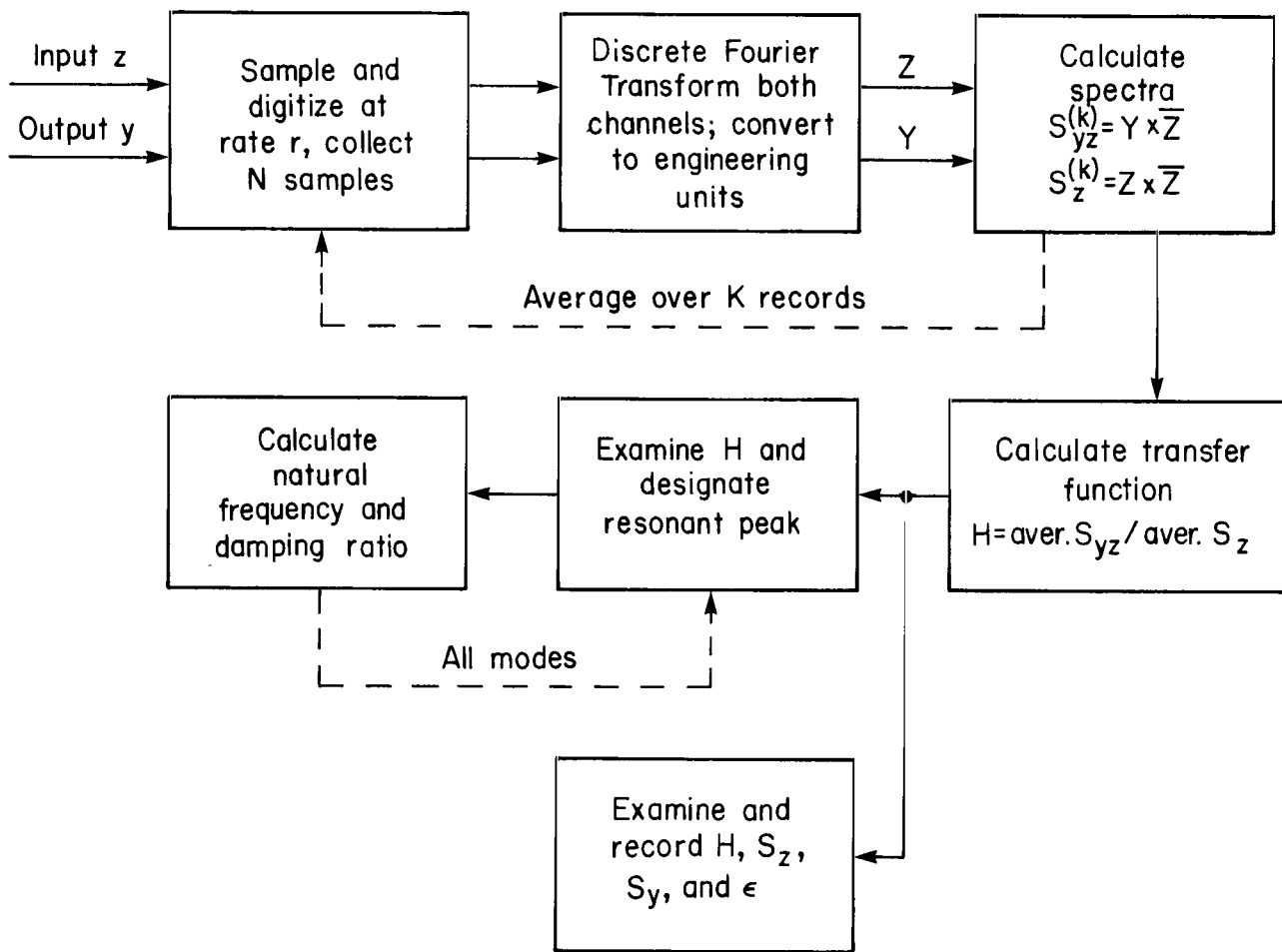


Figure 3.- Outline of dynamic stability measurement procedure based on the transfer function.

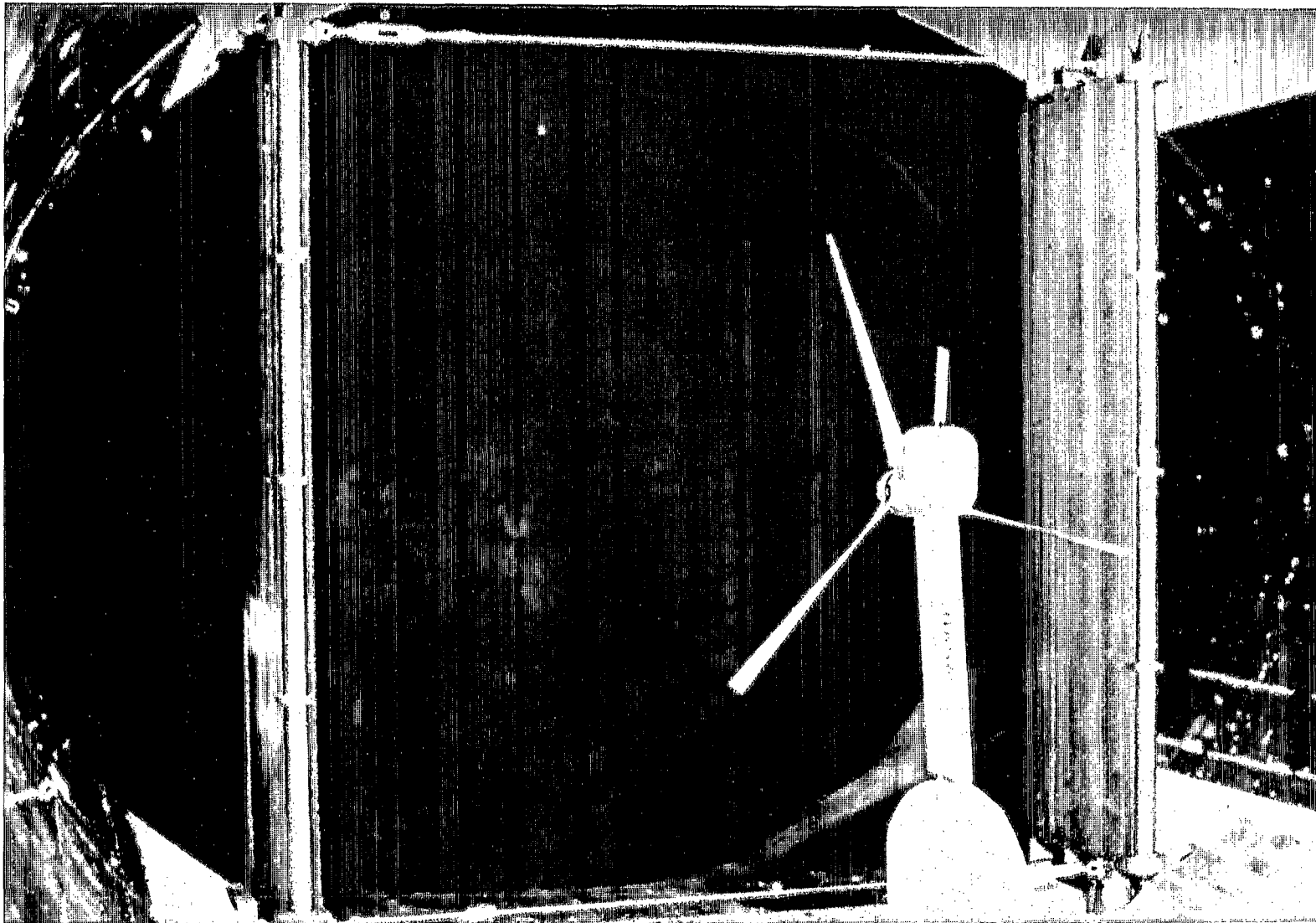
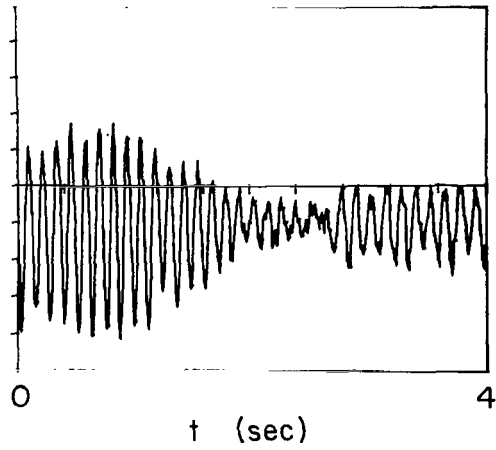


Figure 4.- Proprotor and cantilever wing model in MIT Wright Brothers Wind Tunnel (rotor diameter 0.86 m - note the shaker vane on top of the model).

Wing vertical  
bending  
( $V/\Omega R = .69$ )



Wing chord  
bending  
( $V/\Omega R = .69$ )

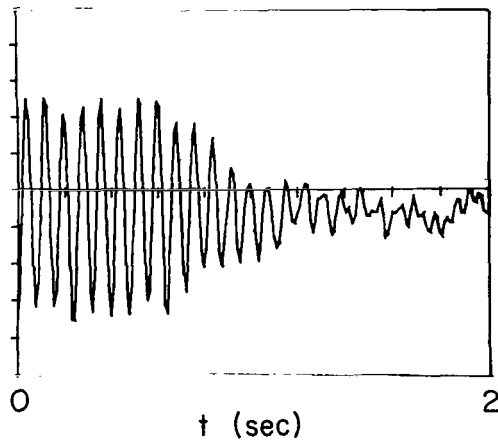
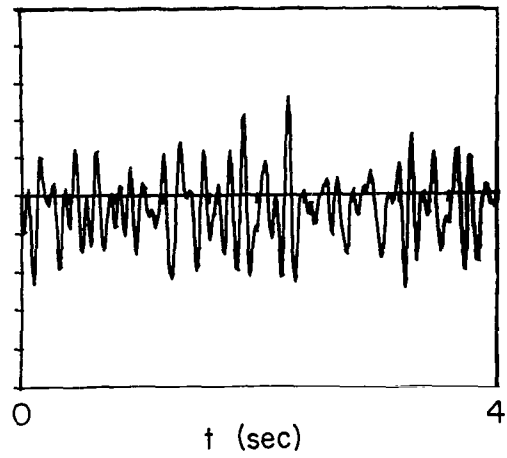


Figure 5.- Examples of transient decay traces for the proprotor and wing model.

Time history



Auto-spectrum

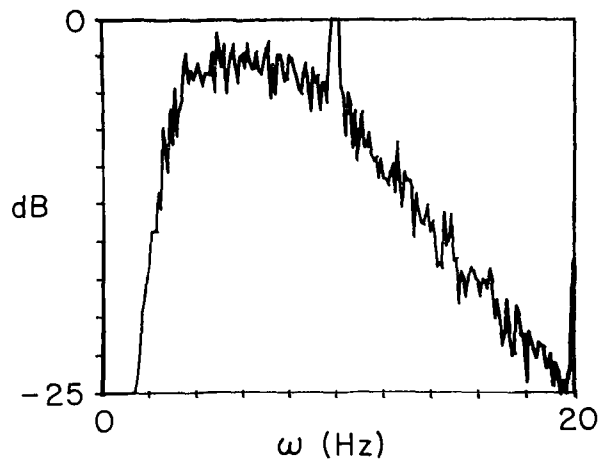


Figure 6.- Time history and autospectrum of input for transfer function measurement.

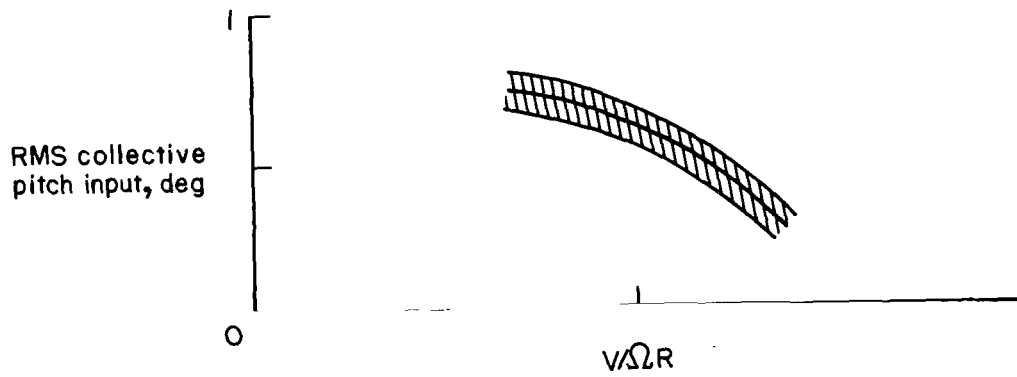
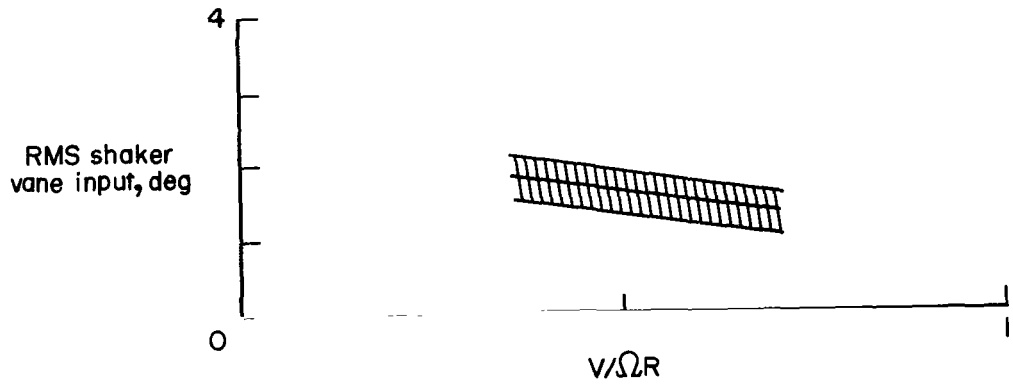


Figure 7.- RMS levels of shaker vane and rotor collective pitch inputs used to excite the model.

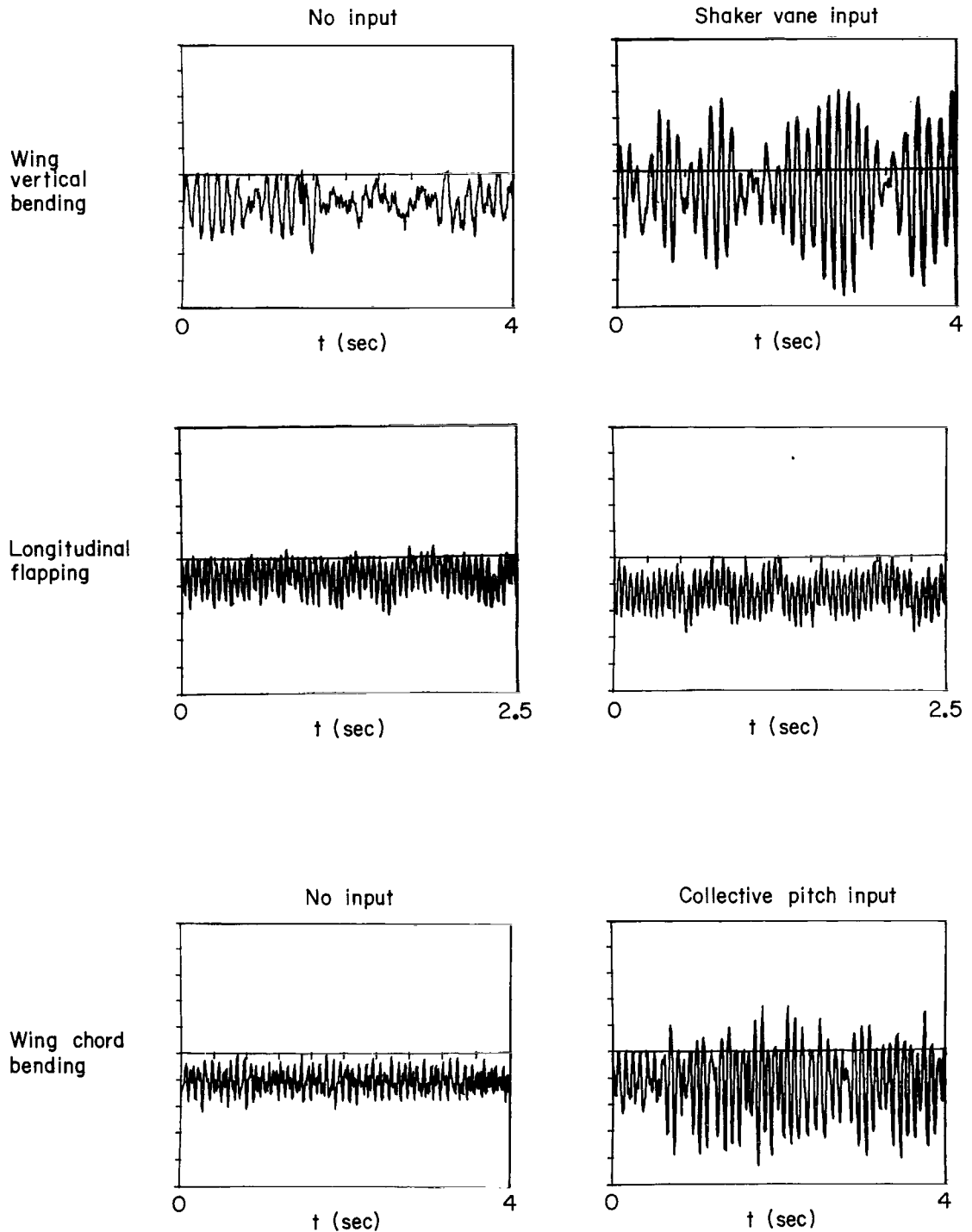


Figure 8.- Time histories of wing and rotor response with no input (wind-tunnel turbulence only) and with external input to excite the model at  $V/\Omega R = 0.69$ .

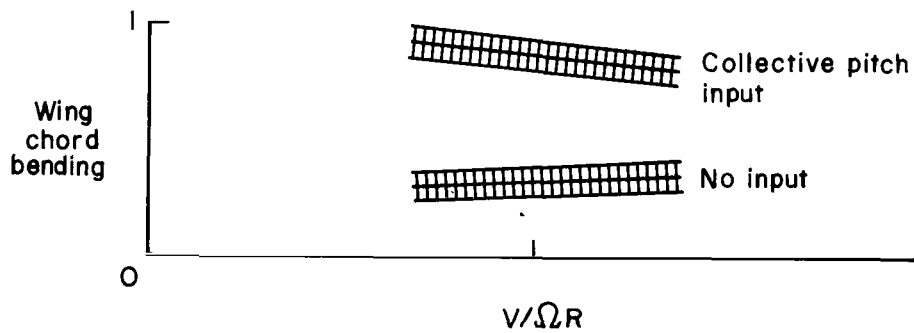
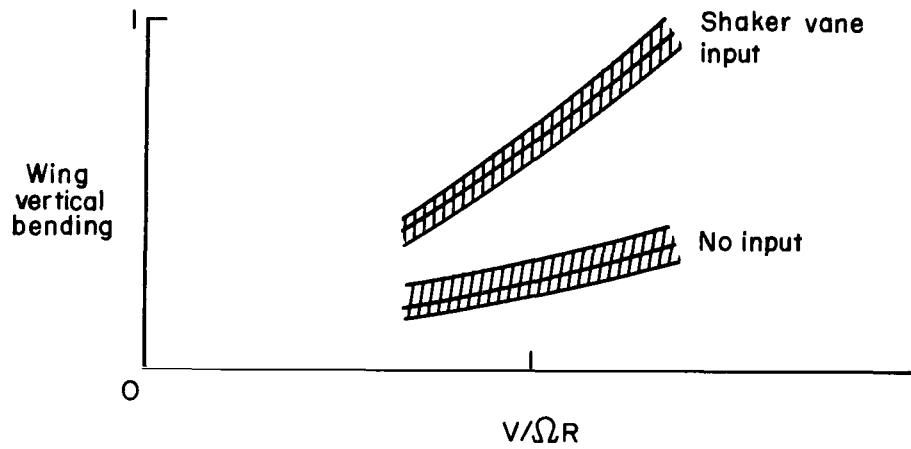


Figure 9.- Levels of wing bending response with and without the external inputs (relative to the maximum response encountered).



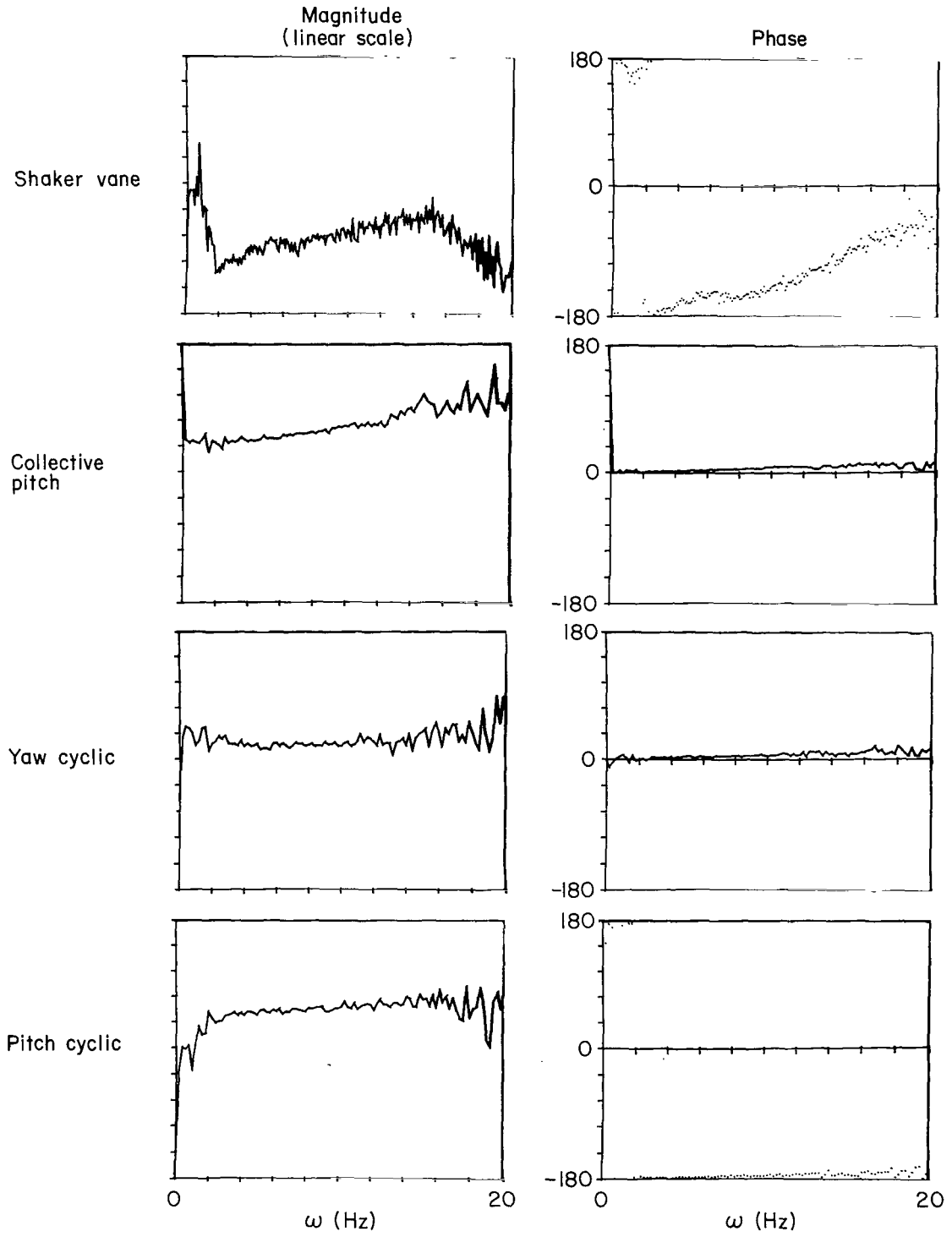


Figure 10.- Transfer functions of the shaker vane and rotor control system actuators.

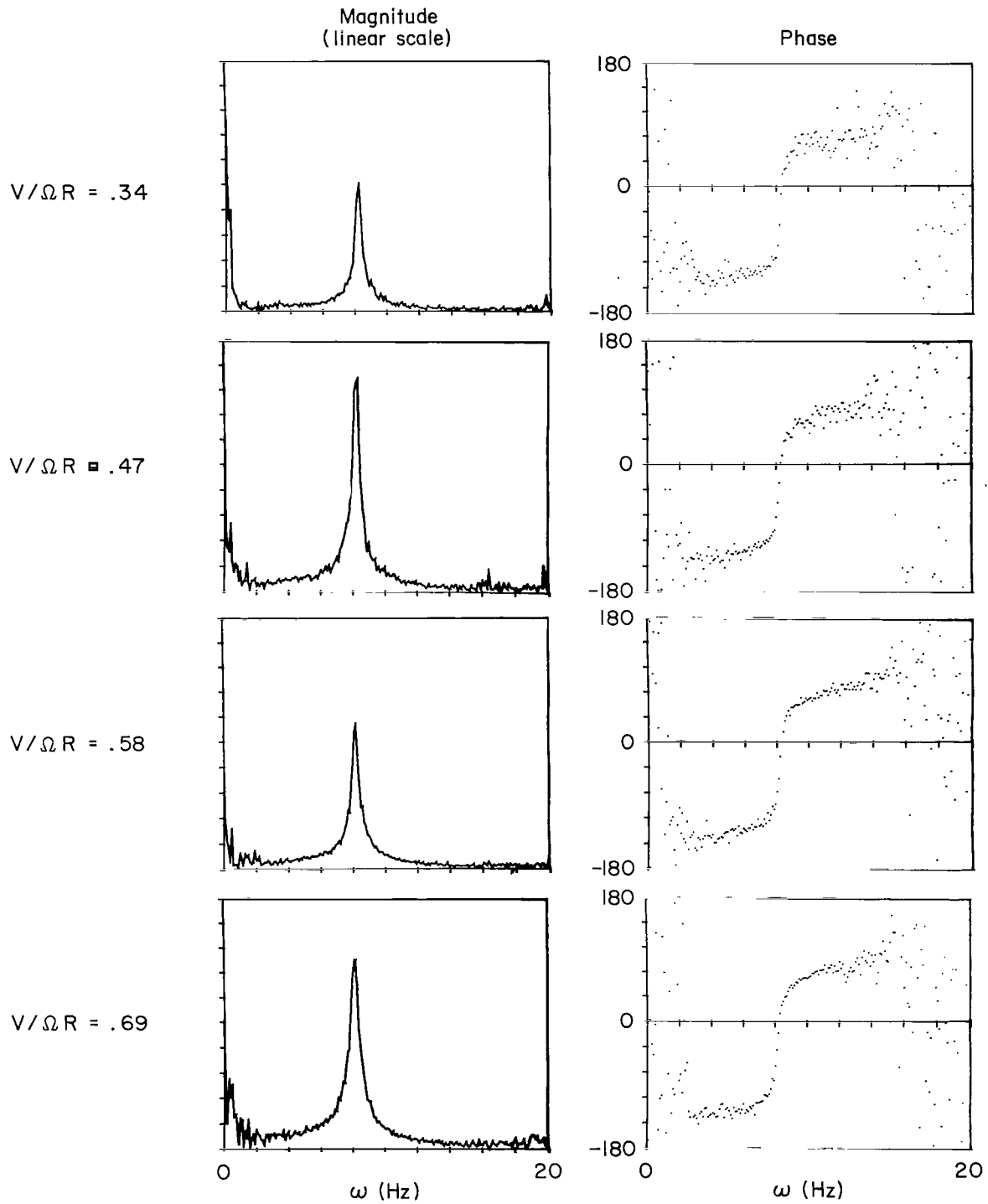


Figure 11.- Measured transfer functions of wing vertical bending response to shaker vane excitation.

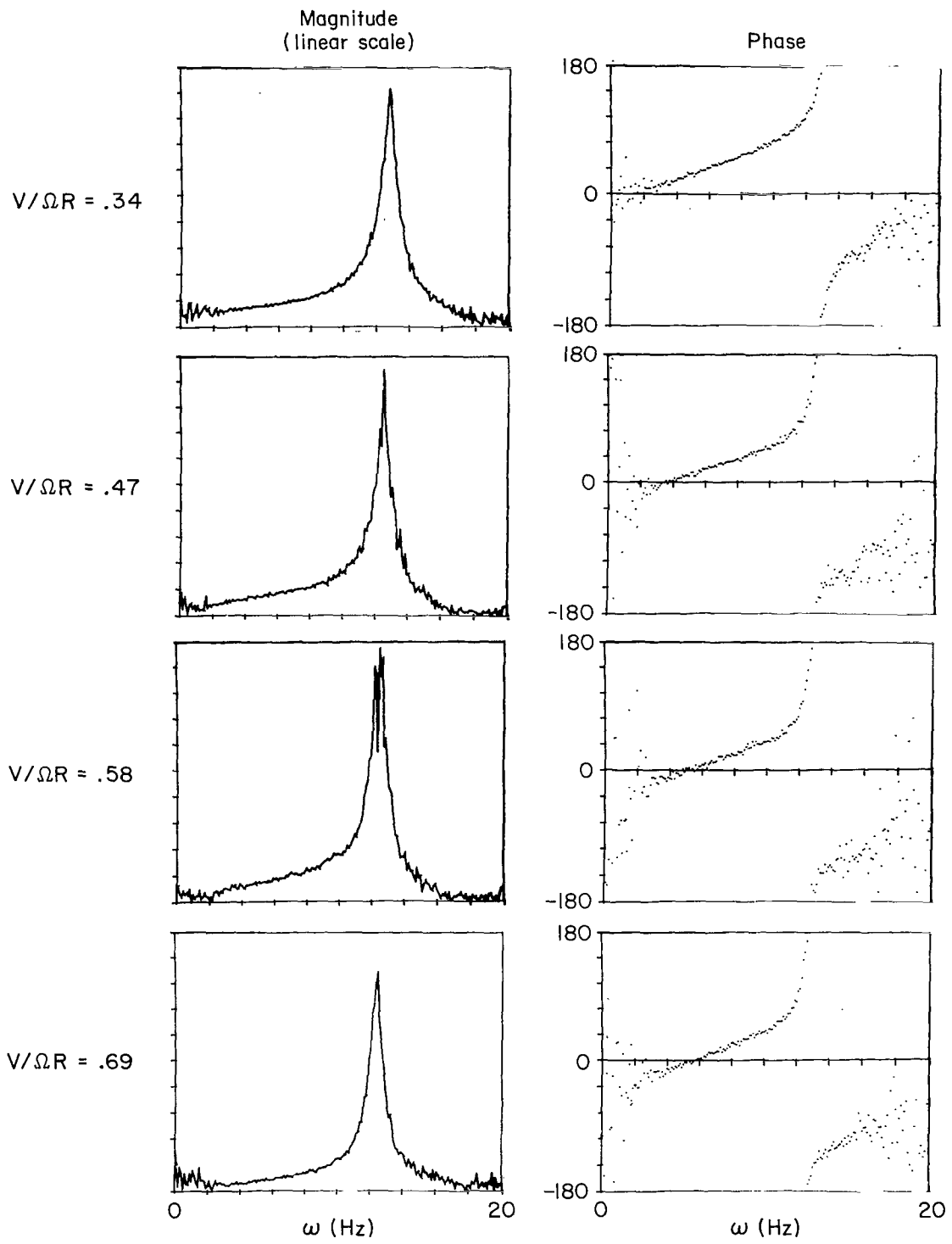


Figure 12.- Measured transfer functions of wing chordwise bending response to collective pitch excitation.

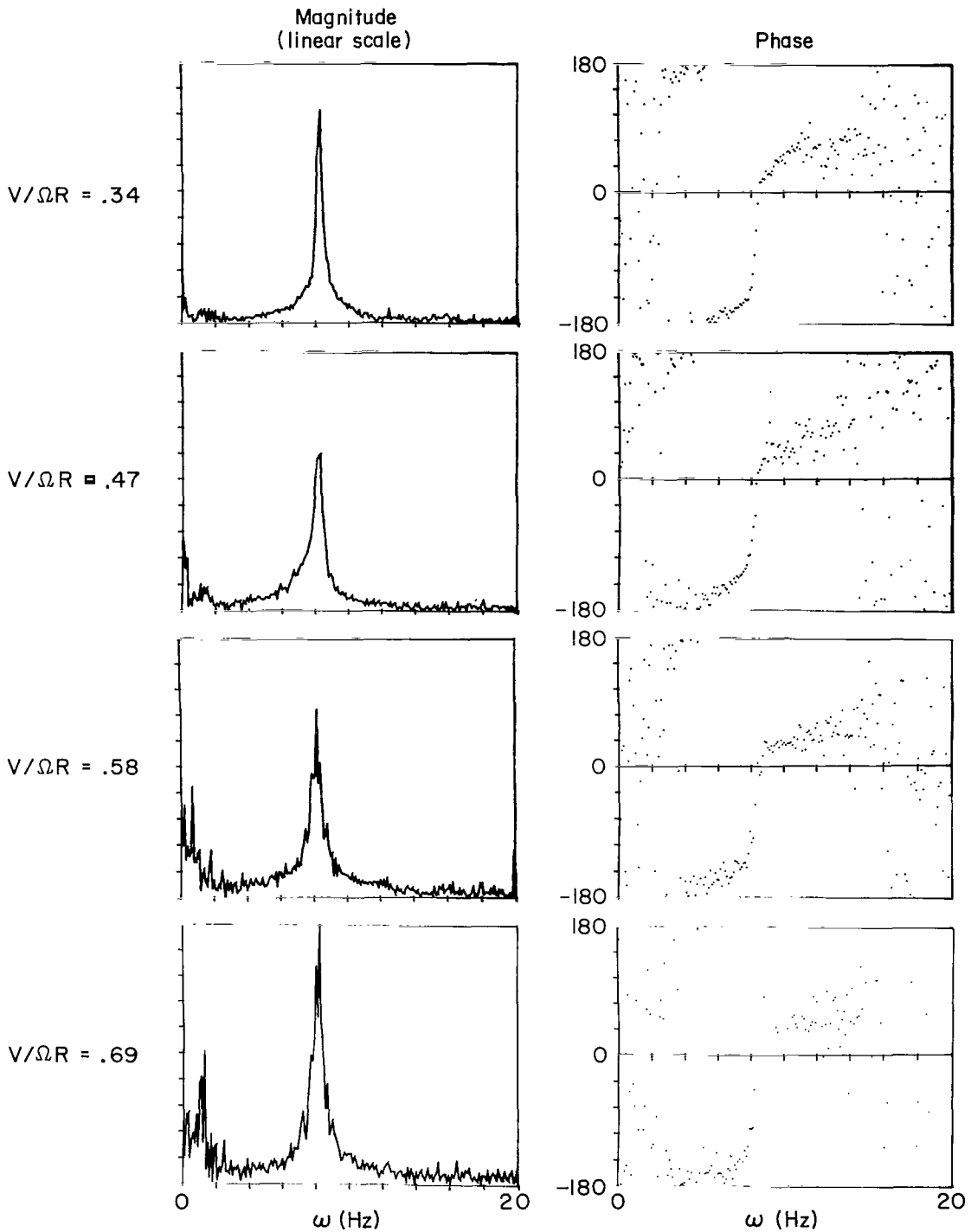
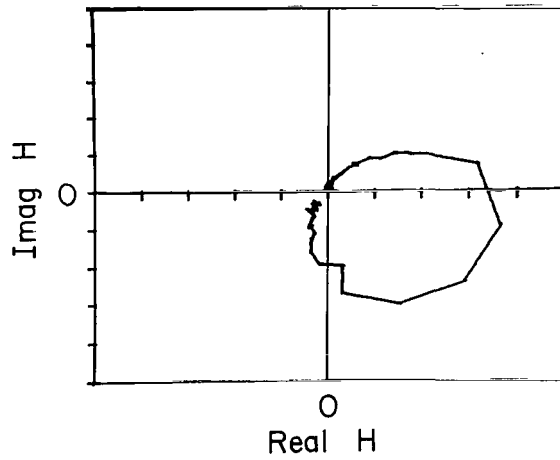


Figure 13.- Measured transfer functions of wing vertical bending response to rotor cyclic pitch excitation.

$$q_1 / \delta_F$$

$$(V/\Omega R = .69)$$



$$q_2 / \theta_0$$

$$(V/\Omega R = .69)$$

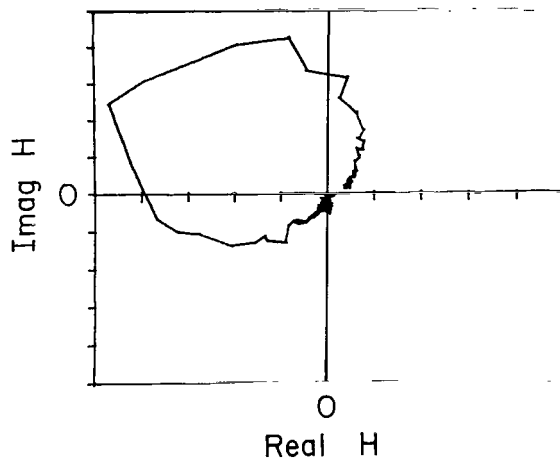
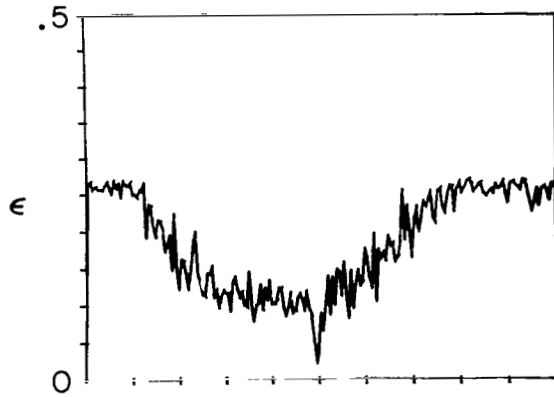


Figure 14.- Typical transfer functions on the phase plane for wing vertical bending response to shaker vane ( $q_1/\delta_F$ ) and for wing chordwise bending response to collective pitch ( $q_2/\theta_0$ ) at  $V/\Omega R = 0.69$ .

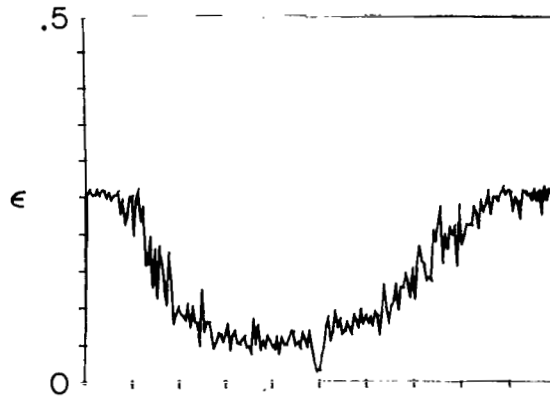
$$q_1 / \delta_F$$

$$(V/\Omega R = .69)$$



$$q_2 / \theta_0$$

$$(V/\Omega R = .69)$$



$$q_1 / \theta_{1C}$$

$$(V/\Omega R = .69)$$

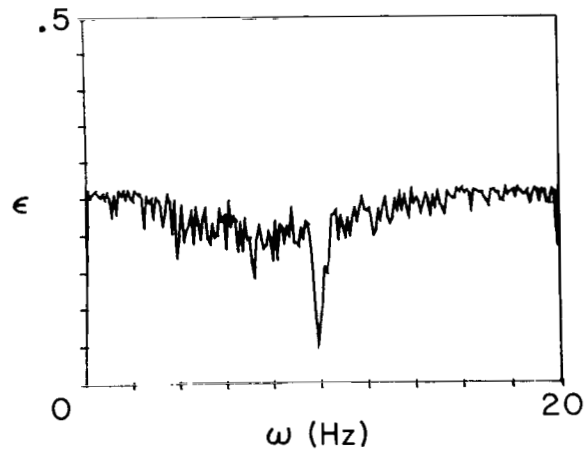


Figure 15.- Transfer function error estimates for wing vertical bending response to shaker vane ( $q_1/\delta_F$ ), for forwardwise bending response to collective pitch ( $q_2/\theta_0$ ), and for wing vertical bending response to rotor cyclic ( $q_1/\theta_{1C}$ ) at  $V/\Omega R = 0.69$ .

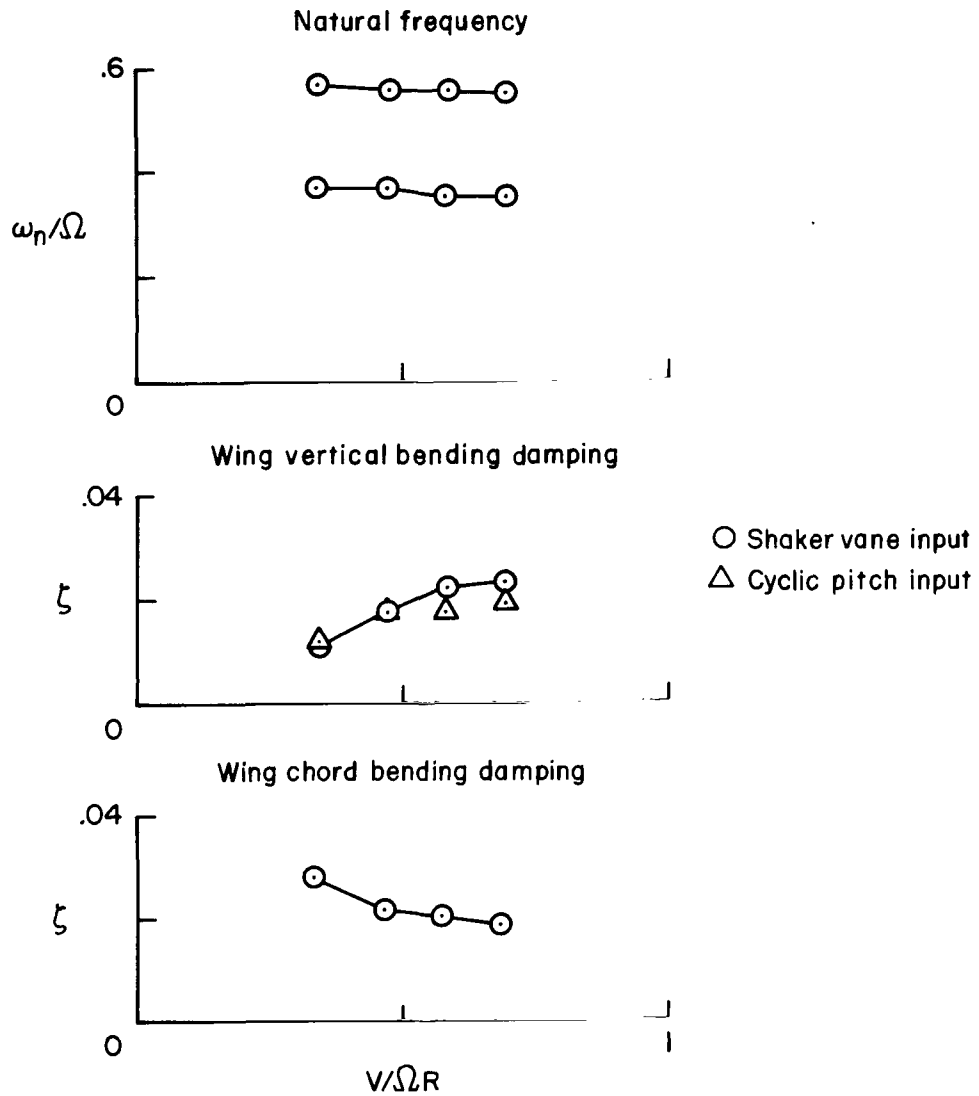


Figure 16.- Natural frequency and damping ratio of the wing vertical and chord-wise bending modes obtained from the transfer function measurements.



463 007 C1 U A 770701 S00903DS  
DEPT OF THE AIR FORCE  
AF WEAPONS LABORATORY  
ATTN: TECHNICAL LIBRARY (SUL)  
KIRTLAND AFB NM 87117

POSTMASTER: If Undeliverable (Section 158  
Postal Manual) Do Not Return

*"The aeronautical and space activities of the United States shall be conducted so as to contribute . . . to the expansion of human knowledge of phenomena in the atmosphere and space. The Administration shall provide for the widest practicable and appropriate dissemination of information concerning its activities and the results thereof."*

—NATIONAL AERONAUTICS AND SPACE ACT OF 1958

## NASA SCIENTIFIC AND TECHNICAL PUBLICATIONS

**TECHNICAL REPORTS:** Scientific and technical information considered important, complete, and a lasting contribution to existing knowledge.

**TECHNICAL NOTES:** Information less broad in scope but nevertheless of importance as a contribution to existing knowledge.

**TECHNICAL MEMORANDUMS:** Information receiving limited distribution because of preliminary data, security classification, or other reasons. Also includes conference proceedings with either limited or unlimited distribution.

**CONTRACTOR REPORTS:** Scientific and technical information generated under a NASA contract or grant and considered an important contribution to existing knowledge.

**TECHNICAL TRANSLATIONS:** Information published in a foreign language considered to merit NASA distribution in English.

**SPECIAL PUBLICATIONS:** Information derived from or of value to NASA activities. Publications include final reports of major projects, monographs, data compilations, handbooks, sourcebooks, and special bibliographies.

**TECHNOLOGY UTILIZATION PUBLICATIONS:** Information on technology used by NASA that may be of particular interest in commercial and other non-aerospace applications. Publications include Tech Briefs, Technology Utilization Reports and Technology Surveys.

*Details on the availability of these publications may be obtained from:*

**SCIENTIFIC AND TECHNICAL INFORMATION OFFICE**

**NATIONAL AERONAUTICS AND SPACE ADMINISTRATION**

**Washington, D.C. 20546**